NASA TECHNICAL NOTE

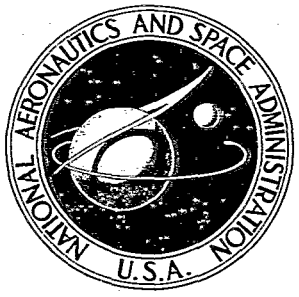

NASA TN D-6498

RELATIVE SUSCEPTIBILITY OF TITANIUM ALLOYS TO HOT-SALT STRESS-CORROSION

by Hugh R. Gray

Lewis Research Center
Cleveland, Ohio 44135

NATIONAL AERONAUTICS AND SPACE ADMINISTRATION • WASHINGTON, D. C. • NOVEMBER 1971

1. Report No.	2. Government Accession No.	3. Recipient's Catalog No.
NASA TN D-6498		

4. Title and Subtitle	5. Report Date
RELATIVE SUSCEPTIBILITY OF TITANIUM ALLOYS TO HOT-SALT STRESS-CORROSION	November 1971
	6. Performing Organization Code

7. Author(s)	8. Performing Organization Report No.
Hugh R. Gray	E-6417
	10. Work Unit No. 129-03

9. Performing Organization Name and Address	11. Contract or Grant No.
Lewis Research Center National Aeronautics and Space Administration Cleveland, Ohio 44135	

12. Sponsoring Agency Name and Address	13. Type of Report and Period Covered
National Aeronautics and Space Administration Washington, D.C. 20546	Technical Note
	14. Sponsoring Agency Code

15. Supplementary Notes

16. Abstract

Susceptibility of titanium alloys to hot-salt stress-corrosion cracking increased as follows: Ti-2Al-11Sn-5Zr-0.2Si(679), Ti-6Al-2Sn-4Zr-2Mo(6242), Ti-6Al-4V(64), Ti-6Al-4V-3Co(643), Ti-8Al-1Mo-1V(811), and Ti-13V-11Cr-3Al(13-11-3). The Ti-5Al-6Sn-2Zr-1Mo-0.25Si(5621S) alloy was both the least and most susceptible depending on heat treatment. Such rankings can be drastically altered by heat-to-heat and processing variations. Residual compressive stresses and cyclic exposures also reduce susceptibility to stress-corrosion. Simulated turbine-engine compressor environmental variables such as air velocity, pressure, dewpoint, salt concentration, and salt deposition temperature have only minor effects. Detection of substantial concentrations of hydrogen in all corroded alloys confirmed the existence of a hydrogen embrittlement mechanism.

17. Key Words (Suggested by Author(s))	18. Distribution Statement
Titanium alloys; Stress-corrosion; Hot-salt stress-corrosion; Hydrogen embrittlement; Turbine-engine environment; Dynamic air environment	Unclassified - unlimited

19. Security Classif. (of this report)	20. Security Classif. (of this page)	21. No. of Pages	22. Price*
Unclassified	Unclassified	58	$3.00

* For sale by the National Technical Information Service, Springfield, Virginia 22151

RELATIVE SUSCEPTIBILITY OF TITANIUM ALLOYS TO HOT-SALT STRESS-CORROSION

by Hugh R. Gray

Lewis Research Center

SUMMARY

The purpose of this investigation was to determine the relative susceptibility to hot-salt stress-corrosion of seven titanium alloys tested in simulated turbine-engine compressor environments. Salt-coated specimens were creep exposed for 100 hours in the temperature range 320° to 480° C (600° to 900° F). Specimens were then tensile tested at room temperature at a constant, low strain rate.

Based on 100-hour crack threshold curves, susceptibility to hot-salt stress-corrosion increased in the following order: Ti-2Al-11Sn-5Zr-0.2Si(679), Ti-6Al-2Sn-4Zr-2Mo(6242), Ti-6Al-4V(64), Ti-6Al-4V-3Co(643), Ti-8Al-1Mo-1V(811), and Ti-13V-11Cr-3Al(13-11-3). The Ti-5Al-6Sn-2Zr-1Mo-0.25Si(5621S) alloy was both the least and most susceptible alloy depending on heat treatment. When the alloys were compared on the basis of their potential use strength (crask threshold stress divided by 0.2 percent creep stress), then the most resistant alloy was the 64, followed by the others listed previously in about the same order. The 5621S alloy ranked just above and below the 811 alloy depending on heat treatment.

It must be emphasized that such rankings can be drastically altered by heat-to-heat and processing variations, as well as by subsequent heat treatments.

Residual compressive stresses and cyclic exposures are the other major variables that reduce susceptibility to stress-corrosion. Simulated compressor environmental variables such as air velocity, pressure, dewpoint, salt concentration, and salt deposition temperature exert only minor effects. Increasing exposures from 100 to 1000 hours decreased crack threshold stresses for all alloys.

Substantial increases in hydrogen concentration of stress-corroded specimens were measured for all alloys. These chemical analyses support a previously proposed concept that corrosion-produced hydrogen is responsible for hot-salt stress-corrosion embrittlement and cracking of titanium alloys.

INTRODUCTION

The phenomenon of hot-salt stress-corrosion of titanium alloys is of interest because of extensive utilization of titanium alloys in gas-turbine engines. Laboratory investigations (refs. 1 and 2) have demonstrated that titanium alloys are susceptible to embrittlement and cracking at elevated temperatures while being stressed in the presence of halides. Conditions of stress, temperature, and salt-air environment which result in hot-salt stress-corrosion in the laboratory can be experienced by compressor components of current engines (ref. 3). Since advanced engine designs specify that titanium alloys operate at even higher stresses and temperatures than called for in current engines, there is concern that hot-salt stress-corrosion might become the limiting factor in the use of titanium alloys. To date, there have not been any reported service failures that could conclusively be attributed to hot-salt stress-corrosion. One of the objectives of this continuing research program at NASA Lewis Research Center has been to determine whether this lack of service failures is indicative of future expectations.

One of the preferred laboratory test techniques for determining susceptibility to hot-salt stress-corrosion involves subjecting salt-coated titanium alloy specimens to static loads. The test temperatures range from 260° to 480° C (500° to 900° F) and the test duration is generally 100 hours. The specimens are then examined for evidence of corrosion or cracking and may be subjected to mechanical testing, such as bend or tensile testing, to determine residual ductility. The results are then interpreted on a stress-corrosion or no-stress-corrosion basis. Thus, the boundary line separating regions of cracking from no cracking or embrittlement from nonembrittlement on a plot of exposure stress against exposure temperature has been termed the threshold curve for hot-salt stress-corrosion.

However, wide variations in published threshold curves exist because of differences in alloys, test conditions, and the criteria used for defining hot-salt stress-corrosion. The author has recently demonstrated (ref. 4) that residual ductility determined by a room-temperature tensile test at a constant, low crosshead speed of 1×10^{-2} centimeter per minute (5×10^{-3} in./min) is a very sensitive technique for determining the occurrence of hot-salt stress-corrosion. Specifically, for the Ti-8Al-1Mo-1V alloy, embrittlement was determined after exposure at 430° C (800° F) at a stress level of about 70 meganewtons per square meter (MN/m^2) (10 ksi). Stress-corrosion cracks were not observed on the fracture surface of specimens until the exposure stress level exceeded 350 MN/m^2 (50 ksi). When the exposure stress was increased to about 580 MN/m^2 (85 ksi), specimens failed during exposure in a brittle manner. These results (ref. 5) demonstrate that there are at least three different criteria that can be used to define a 100-hour threshold curve for hot-salt stress-corrosion: embrittlement, cracking, and

brittle rupture. For the Ti-8Al-1Mo-1V alloy, significant differences exist among threshold curves defined by these three criteria.

Another variable that has been almost completely ignored by prior investigators is the influence of specimen surface condition. The author has demonstrated (ref. 6) that significant differences exist between both embrittlement and crack threshold curves for Ti-8Al-1Mo-1V alloy specimens in the as-machined and stress-relieved surface conditions. This effect is largely a result of the beneficial influence of residual compressive stresses in the surface material on the bore of the tubular specimens. Of course, some types of machining operations could introduce residual tensile stresses in specimens of different configurations. In those instances, the threshold curve for specimens with residual tensile surface stresses could be expected to occur at lower stress levels than if the same specimens were in the stress-relieved condition. The investigation of reference 6 demonstrated that variations in residual surface stresses, which result from differences in specimen surface preparation, could contribute to the significant variations reported for literature threshold curves for various titanium alloys.

The purpose of the present investigation was to determine the relative susceptibility of various titanium alloys to hot-salt stress-corrosion. It is important to note that most of the titanium alloys included in this program are commercially available. They include both widely used alloys developed several years ago and more recently developed high creep strength alloys. One experimental alloy is also included. The alloys were usually tested in commonly used commercial heat-treated conditions. The exposure conditions simulated the environment normally encountered in the compressors of current jet-turbine engines. Specimens of the titanium alloys were tested in a dynamic air facility at an air velocity of 340 meters per second (1100 ft/sec), an absolute air pressure of 0.2 MN/m^2 (30 psi), and an air dewpoint of -84° C (-120° F). Specimens were also tested in static air laboratory furnaces. Hence, the influence of air velocity could be readily ascertained. The influence of specimen surface condition was also determined by testing specimens in both the as-machined and chemically milled (stress-relieved) conditions. Both embrittlement and crack threshold curves were usually determined for all alloys. Standard vacuum fusion chemical analyses were made on selected stress-corroded specimens.

MATERIALS, SPECIMENS, AND PROCEDURE

Materials

Seven titanium alloys were used in this investigation. Six of these alloys were obtained from commercial vendors and one experimental alloy was obtained from an independent laboratory. The six commercial alloys are the following: titanium - 8 aluminum - 1 molybdenum - 1 vanadium (811), titanium - 6 aluminum - 4 vanadium

(64), titanium - 6 aluminum - 2 tin - 4 zirconium - 2 molybdenum (6242), titanium - 2 aluminum - 11 tin - 5 zirconium - 0.2 silicon (679), titanium - 13 vanadium - 11 chromium - 3 aluminum (13-11-3), and titanium - 5 aluminum - 6 tin - 2 zirconium - 1 molybdenum - 0.25 silicon (5621S). The experimental alloy was titanium - 6 aluminum - 4 vanadium - 3 cobalt (643).

Vendor certified chemical analyses of these alloys are presented in table I. The vendor, heat number, bar size, and certified mechanical properties of the as-received alloys are reported in table II.

A complete listing of all heat treatments performed by the vendors and by NASA

TABLE I. - VENDOR CERTIFIED CHEMICAL ANALYSES OF TITANIUM ALLOY INGOTS (WEIGHT PERCENT)

Alloy	Al	Sn	Zr	Mo	V	Si	Cr	Co	Fe	N	C	O	H
811	7.8	----	----	1.0	1.0	----	----	----	0.05	0.011	0.023	0.07	0.0070
64	6.4	----	----	----	4.1	----	----	----	.13	.015	.021	.14	.0050
6242	6.3	2.0	3.8	2.0	----	----	----	----	.07	.009	.01	.098	.0070
679	2.3	10.7	4.7	----	----	0.18	----	----	.06	.008	.023	.14	.0066
5621S (1)	5.0	6.4	1.9	.92	----	.28	----	----	.03	.006	.02	.10	.0056
5621S (2)	5.2	5.9	1.9	.84	----	.27	----	----	.05	.009	.02	.113	.0036
643	6.5	----	----	----	3.9	----	----	3.3	.05	.012	-----	.15	------
13-11-3	3.0	----	----	----	13.4	----	10.5	----	.13	.026	.018	.12	.0104

TABLE II. - VENDOR CERTIFIED MECHANICAL PROPERTIES OF TITANIUM ALLOYS

Alloy	Vendor	Heat	Bar diameter		0.2 Percent yield strength		Tensile strength		Reduction of area, percent	Elongation, percent
			cm	in.	MN/m^2	ksi	MN/m^2	ksi		
811	TMCA	G-500	2.5	1	980	142	1020	148	40	20
64	TMCA	G-5858	1.9	.75	1020	148	1070	155	40	18
6242	Reactive Metals	293180	1.9	.75	970	141	1040	151	45	16
679	TMCA	G-6360	1.9	.75	1020	148	1100	159	45	20
5621S (1)	Reactive Metals	294204	1.3	.50	1000	145	1090	158	33	12
5621S (2A)	Reactive Metals	303021	3.3	1.3	850	124	990	143	19	11
5621S (2B)	Reactive Metals	303021	3.3	1.3	870	126	1000	145	21	12
643	TMCA - Battelle	Experimental	2.2	.86	1580	230	1720	250	12	6
13-11-3	TMCA	D-4514	1.9	.75	1110	161	1230	178	19	10

TABLE III. - TITANIUM ALLOY HEAT TREATMENTS AND MECHANICAL PROPERTIES[a]

Alloy	Heat treatment	Tensile strength		Fracture strength		Reduction of area, percent	Elongation, percent
		MN/m^2	ksi	MN/m^2	ksi		
811 Mill anneal/air cool	As-received: 790° C (1450° F), 1 hr, air cool	1030	150	930	135	33	18
811 Mill anneal/furnace cool	900° C (1650° F), 1 hr, furnace cool	1030	149	940	137	33	21
811 Duplex	650° C (1200° F), 24 hr, AC	1070	155	970	140	34	21
811 Triplex	1010° C (1850° F), 1 hr, AC + 590° C (1100° F), 8 hr, AC	960	139	880	128	35	23
64 Mill anneal	As-received: 840° C (1550° F), 2 hr, FC to 700° C (1300° F), 2 hr, AC	1070	155	970	140	27	16
64 Duplex	930° C (1700° F), 1 hr, water quench + 540° C (1000° F), 4 hr, AC	1170	169	1030	150	30	14
6242 Mill anneal	As received: 900° C (1650° F), 1 hr, AC	1120	162	980	142	33	18
6242 Duplex	970° C (1775° F), 1 hr, AC + 590° C (1100° F), 8 hr, AC	1020	148	920	133	35	21
679 Mill anneal	As-received: 700° C (1300° F), 2 hr, AC	1030	149	900	131	34	22
679 Duplex	900° C (1650° F), 1 hr, AC + 500° C (930° F), 24 hr, AC	1050	152	950	138	31	19
5621S (1)	As-received: 980° C (1800° F) roll, 980° C (1800° F), 1 hr, AC + 590° C (1100° F), 2 hr, AC	1080	156	970	141	34	17
5621S (2A)	As-received: 980° C (1800° F) roll, 1040° C (1900° F), 1 hr, AC + 590° C (1100° F), 2 hr, AC	1100	160	1030	150	25	16
5621S (2B)	As-received: 1040° C (1900° F) roll, 1040° C (1900° F), 1 hr, AC + 590° C (1100° F), 2 hr, AC	1100	159	1090	158	14	11
5621S (2C)	(2B) + 980° C (1800° F), 1 hr, AC + 590° C (1100° F), 2 hr, AC	1070	155	1060	154	18	14
643 Duplex	As-received: 920° to 780° C (1690° to 1435° F) roll, 840° C (1550° F), 1 hr, WQ + 480° C (900° F), 2 hr, AC	1550	225	1550	225	6	3
13-11-3 Duplex	As-received: 790° C (1450° F), 1/4 hr, WQ + 480° C (900° F), 22 hr, AC	1290	187	1260	183	18	14

[a]NASA Lewis, tubular specimens.

together with mechanical properties determined on the tubular specimens used in this investigation are presented in table III. All of the alloys except the 13-11-3 and 643 were stress-corrosion tested in the as-received (mill anneal (MA)) condition and in various other heat-treated conditions. Most of these heat treatments are commonly encountered in various aerospace and industrial applications.

The 811, 6242, 679, and 5621S alloys are generally referred to as near-alpha or superalpha alloys. The 64 and 643 alloys are alpha plus beta types and the 13-11-3 is a beta alloy. Photomicrographs of all of the as-received and heat-treated alloys are given in figure 8 at the back of the report. These alloys were etched with hydrofluoric and nitric acid mixtures. All of these structures are typical and representative of normal material processed and annealed in the alpha plus beta phase field with the exception of the 13-11-3 and 5621S alloys. The 13-11-3 alloy was processed and annealed above the beta transus, as evident from the structure shown in figures 8(r) and (s). The 5621S (2) alloy was processed and/or annealed above the beta transus, as evident from figures 8(ℓ) to (p).

Specimens

Tubular tensile specimens of the type illustrated in figure 1 were employed in this investigation. Specimens with subsize heads were used for the 5621S and 643 alloys because of the limited quantity or diameter of the bar stock. The specimens were machined from the as-received and/or heat-treated bar stock. One series of as-machined specimens was cleaned with acetone and distilled water immediately prior to salting and stress-corrosion testing. Another series of as-machined specimens was stress relieved by chemical milling (ref. 6) in a solution of 3-percent hydrofluoric acid, 30-percent nitric acid, and 67-percent water. Approximately 0.002 centimeter

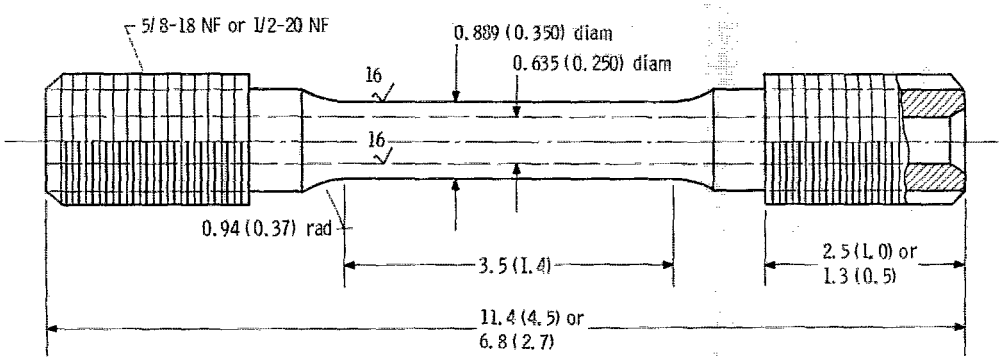

Figure 1. - Tubular, titanium alloy specimens used in this investigation. (All dimensions are in cm (in.).)

(0.001 in.) of metal was removed from all surfaces of these specimens. This chemical dissolution process should not be confused with electrochemical milling or electropolishing techniques.

Test Procedure

Salt coating. - All of the test specimens were precoated with chemically pure sodium chloride immediately prior to stress-corrosion testing. The average coating amounted to about 0.1 milligram per square centimeter (0.6 mg/in.^{2}). This concen-

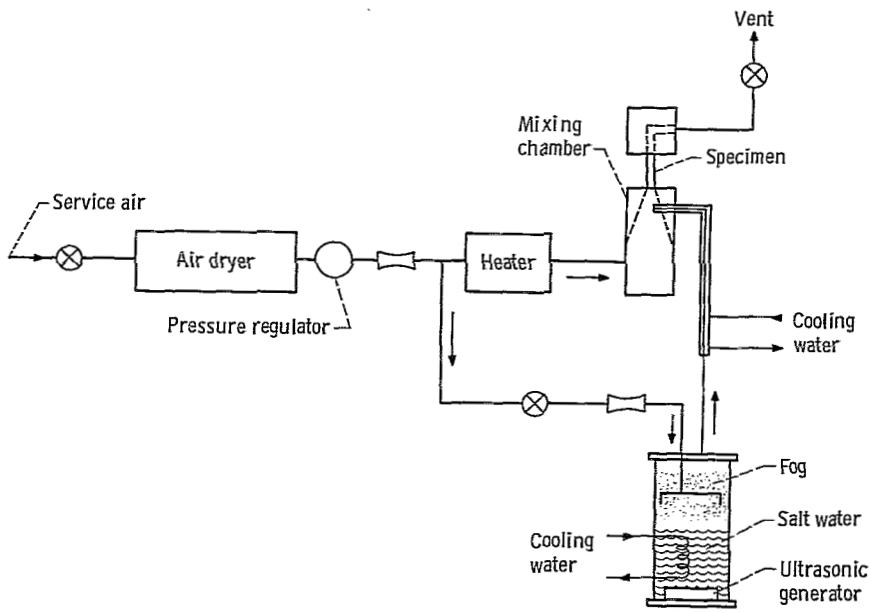

(a) Apparatus for presalting unstressed specimens.

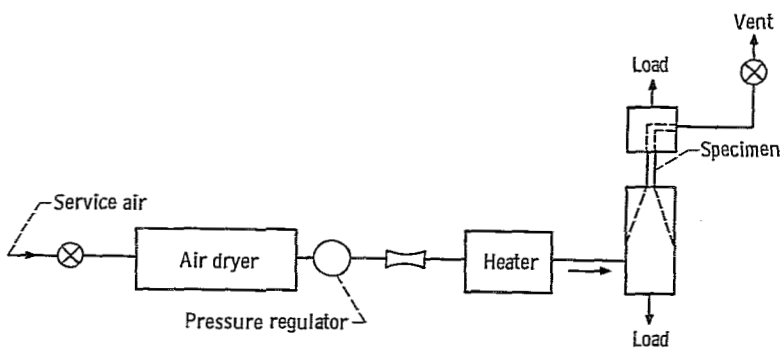

(b) Apparatus for stress-corrosion exposure of presalted specimens.

Figure 2. - Hot-salt stress-corrosion apparatus which simulates turbine-engine compressor environment.

tration was within the range measured on service airfoils (ref. 7). The salt was uniformly deposited on the bore of unstressed specimens at 200° C (400° F) in the dynamic air salting apparatus illustrated in figure 2(a). Details of the salting technique and the dynamic air apparatus can be found in references 8 and 9.

Stress-corrosion exposure. - Subsequent to being coated with salt, one series of specimens was exposed to static air in standard laboratory creep furnaces. This environment was essentially stagnant since the ends of the tubular specimens were sealed by the loading train. Another series of specimens was exposed to salt-free air in the dynamic air apparatus shown in figure 2(b). The air velocity over the range of temperatures used was about 340 meters per second (1100 ft/sec) (Mach 0.7). The absolute air pressure was 0.2 MN/m^2 (30 psi) and the air dewpoint at -84° C (-120° F).

Specimens were usually exposed for approximately 96 hours in the temperature range 320° to 480° C (600° to 900° F). The influence of exposure time was studied by exposing a limited number of alloy specimens for 240 and 1000 hours. The stresses applied ranged from 70 to 830 MN/m^2 (10 to 120 ksi). The amount of creep that occurred during the exposure was determined by measuring the change in outer diameter of the specimens and calculating the apparent change in area. These creep measurements were used only as an approximate check of the literature values of the 0.2 percent - 100 hour creep stresses used for normalizing threshold stresses. A few specimens failed during the stress-corrosion exposure period because of either overloading or severe stress-corrosion cracking.

Tensile testing. - All specimens that had not failed during exposure were tensile tested at room temperature at a constant crosshead speed of 0.01 centimeter per minute (0.005 in./min). These tensile testing conditions had been determined to provide high sensitivity to embrittlement resulting from stress corrosion and were also reasonably convenient to apply (ref. 4). Elongation was measured over a 2.54-centimeter (1.00-in.) gage length. Apparent reduction of area data were determined from changes of only the outside diameter of the tubular specimens. A complete listing of all test conditions and results is contained in tables V to XVIII which appear at the back of the report.

Interpretation of hot-salt stress-corrosion damage. - Any specimen exhibiting residual elongation less than 15 percent and residual reduction of area less than 25 percent was arbitrarily classified as embrittled. The embrittlement threshold curve was drawn below the data points meeting this criterion of reduced ductility.

A second criterion of stress-corrosion damage was also used. The fracture surface of each specimen was examined under a microscope at ×30 for evidence of stress-corrosion cracking. Cracks as small as 0.002 centimeter (0.001 in.) deep could be easily identified because they were covered with oxides and corrosion products. This type of cracking definitely occurred during the hot-salt stress-corrosion exposure but usually at exposure stress levels greater than that required for embrittlement. The

crack threshold curve was drawn below the data points for specimens with cracks evident on the fracture surface.

The brittle rupture criterion discussed in the INTRODUCTION was not used in this investigation.

Measurement of deposited salt. - Concentrations of deposited salt were measured on the bore of each of the fractured specimens. The reported concentrations represent the average of the values measured on each of the two broken portions. These measurements were made with a commercially available, chemical titration technique for soluble chlorides (ref. 10).

Hydrogen analyses. - Standard vacuum fusion chemical analyses for hydrogen content were made on selected specimens by an outside laboratory. Small samples (0.05 g) were cut from regions immediately adjacent to the fracture surfaces of the broken portions of the specimens. This size sample represents the minimum size required by the vendor for accurate analysis. Repeated analyses of the as-received 811 alloy (70 ppm) indicated the vendor's precision to be about ±15 ppm.

RESULTS AND DISCUSSION

Relative Susceptibility of Titanium Alloys

The relative susceptibility to hot-salt stress-corrosion of the seven alloys in the various heat-treated conditions studied can be seen in figure 3. The individual threshold curves for each of these alloys for all test conditions considered are presented in figures 9 to 21, which appear at the back of the report.

Alloy susceptibility to hot-salt stress-corrosion increased in the following order: 679, 6242, 64, 643, 811, and 13-11-3. The 5621S alloy in different heat treatments was both the least and most susceptible alloy.

Specimens in the chemically milled surface condition were used for this ranking so that alloy susceptibility was not masked by the effects of residual machining stresses. Crack threshold curves were used for these comparisons because three of the alloys (643, 13-11-3, and 5621S) exhibited relatively low ductility in either the as-received, heat treated, or unsalted exposed conditions. Since the ductility of these alloys without salted exposure was less than the arbitrary, residual ductility criterion discussed in the Test Procedure section, an embrittlement threshold curve is not applicable for these alloys.

Standard thresholds. - It is evident from the crack threshold curves shown in figure 3(a) that the 679 and 6242 alloys are the most resistant of all the alloys tested. The threshold curves for both the mill anneal and duplex anneal conditions of the 679 and 6242

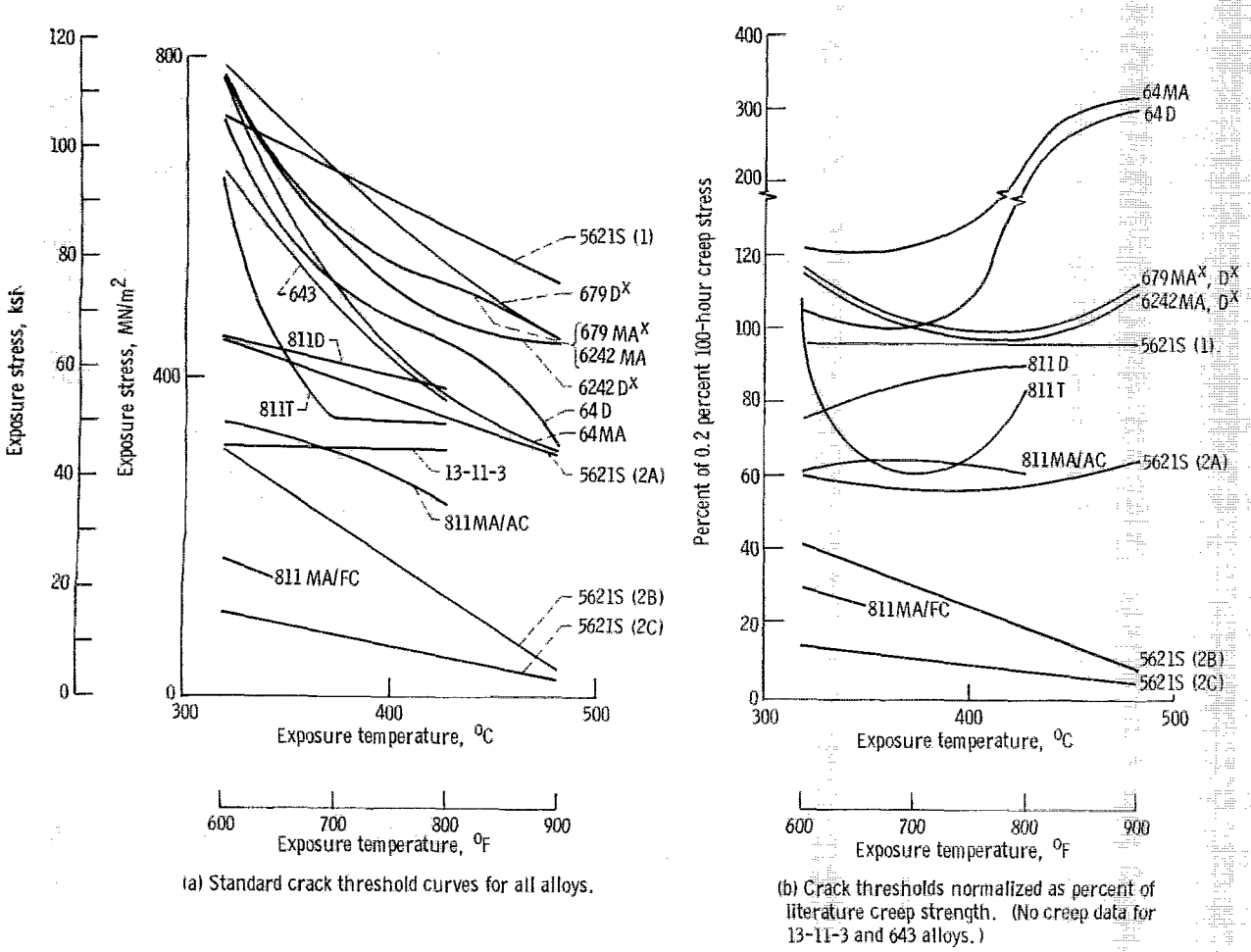

(a) Standard crack threshold curves for all alloys.

(b) Crack thresholds normalized as percent of literature creep strength. (No creep data for 13-11-3 and 643 alloys.)

Figure 3. - 96-Hour crack threshold curves for alloys investigated. (Chemically milled specimens, dynamic air (x, static air).)

alloys are all essentially equivalent. For example, both conditions of each alloy exhibited cracking at an exposure stress of about 790 MN/m^2 (115 ksi) at 320^o C (600^o F), and about 450 MN/m^2 (65 ksi) at 480^o C (900^o F).

The 64 alloy also exhibited good resistance to hot-salt stress-corrosion cracking in both the mill anneal and duplex anneal conditions. However, the exposure stress levels necessary for cracking were lower than those for the 679 and 6242 alloys over the entire temperature range investigated. For instance, the exposure stress required for cracking at 320^o C (600^o F) was about 760 MN/m^2 (110 ksi) and at 480^o C (900^o F) was about 310 MN/m^2 (45 ksi). The crack threshold curve for the 643 alloy was parallel to, but about 70 MN/m^2 (10 ksi) less than, the threshold curve for the 64 duplex alloy over the temperature range 320^o to 430^o C (600^o to 800^o F).

The 13-11-3 alloy was quite susceptible to stress-corrosion cracking. The crack threshold curve for this alloy occurred at about 310 MN/m^2 (45 ksi) over the temperature range 320^o to 430^o C (600^o to 800^o F).

The susceptibility of the 811 alloy varied markedly for the four heat-treated conditions considered. For example, the triplex condition resulted in good resistance to cracking with the threshold stress at 650 MN/m^2 (95 ksi) at 320° C (600° F) and 350 MN/m^2 (50 ksi) at 430° C (800° F). The threshold for the duplex condition decreased from 440 to 380 MN/m^2 (65 to 55 ksi) over the same temperature range. However, the mill anneal condition was substantially inferior to both the triplex and duplex conditions. The resistance of the 811 alloy could also be affected by another heat treating variable - cooling rate. For example, chemically milled specimens in the mill anneal/air cooled condition exhibited a threshold curve that decreased from about 350 to 240 MN/m^2 (50 to 35 ksi) over the temperature range 320° to 430° C (600° to 800° F). For comparison, chemically milled specimens in the mill anneal/furnace cooled condition exhibited a threshold stress of only 170 MN/m^2 (25 ksi) at 320° C (600° F).

The 5621S alloy exhibited the widest range of susceptibility of all the alloys tested in this program. The 5621S (1) condition ($\alpha+\beta$ roll, $\alpha+\beta$ anneal) exhibited resistance to cracking superior to that of any alloy studied in this investigation. Its threshold curve decreased from 720 to 510 MN/m^2 (105 to 75 ksi) at 320° to 480° C (600° to 900° F). However, when the discontinuous alpha microstructure was altered by either β rolling or β annealing, susceptibility to cracking increased dramatically. For example, the 5621S (2A) condition ($\alpha+\beta$ roll, β anneal) resulted in a threshold curve that decreased from 440 to 310 MN/m^2 (65 to 45 ksi) at 320° to 480° C (600° to 900° F). Susceptibility increased still more for the 5621S (2B) condition (β roll, β anneal) as the threshold curve decreased from 310 to 35 MN/m^2 (45 to 5 ksi) over the same temperature range. The 5621S (2C) condition (β roll, β anneal, $\alpha+\beta$ anneal) was the least resistant alloy tested in this program. Its threshold curve decreased from 100 to about 35 MN/m^2 (15 to 5 ksi).

Normalized thresholds. - Another, and perhaps more meaningful, basis for comparing the susceptibility of these alloys is to consider the crack threshold stress as a percentage of the potential use strength of the alloy. Since creep strength is usually the limiting design factor in the use of titanium alloys for compressor applications, handbook values of the 0.2 percent - 100 hour creep stress for each alloy and heat treatment were selected as the normalizing factor. Such a plot of the crack threshold stress as a percentage of the creep stress of the alloy against exposure temperature is given in figure 3(b). This method of evaluating resistance to hot-salt stress-corrosion cracking yields some valuable information. For instance, although the threshold curves for both 64 mill anneal and duplex occurred at intermediate stress levels in figures 3(a), these stresses are in fact as much as three times the creep strength of the alloy. Hence, on this basis, the resistance to hot-salt stress-corrosion cracking of the 64 alloy is far superior to all other alloys tested in this investigation.

The 679 and 6242 alloys in both the mill anneal and duplex conditions were essentially equivalent with their threshold curves occurring at about 100 percent of the creep

strength over the entire temperature range of exposure. The 811 alloy once again exhibited large variations in threshold curves for the various heat treatments studied. The threshold for the 811 triplex ranged from 60 to 100 percent, while the 811 duplex ranged from 75 to 90 percent of the creep strength. The threshold for the 811 mill anneal/air cooled condition occurred at 60 percent while the threshold curve for the furnace cooled condition decreased from about 30 to an estimated 0 percent of the creep strength of the alloy. The 5621S alloy also exhibited large variations in threshold curves for the four conditions tested. The threshold stress was about 100 percent of the creep stress for condition (1) ($\alpha+\beta$ roll, $\alpha+\beta$ anneal) and about 60 percent for condition (2A) ($\alpha+\beta$ roll, β anneal) over the entire temperature range investigated. However, for conditions (2B) (β roll, β anneal) and (2C) (β roll, β anneal, $\alpha+\beta$ anneal), threshold stresses decreased from 40 to 5 percent and 15 to 5 percent of the creep stress, respectively, as the exposure temperature increased from 320° to 480° C (600° to 900° F).

Neither the 643 nor the 13-11-3 alloys could be accurately evaluated on this basis because creep strength data are not available from the literature. The limited creep data determined in this investigation during stress-corrosion exposure indicated that for both of these alloys cracking occurred below the creep strength at 320° C (600° F) but somewhat above the creep strength at 430° C (800° F) (see tables XVI and XVII).

Effect of Microstructural and Processing Variables

It is tempting to rationalize the relative susceptibility of the alloys studied in this investigation according to chemical composition. Specifically, several previous investigators have ranked the stress-corrosion susceptibility of titanium alloys according to aluminum content (refs. 11 and 12), aluminum plus oxygen (refs. 13 to 15), and beta stablizer content (refs. 15 to 17). Usually, the lower the aluminum and/or oxygen, or the higher the beta stabilizer content, the more resistant the alloy is to hot-salt and salt water stress-corrosion. Although these schemes may have merit, the results obtained in this investigation demonstrating the wide range of susceptibility exhibited by a single alloy (e.g., 811 or 5621S) indicate that caution must be exercised when ranking alloys. Specifically, the dramatic influence of both processing variables and subsequent heat treatments and the resulting microstructural variations must be considered.

Microstructure-susceptible alloys. - Although a full evaluation of microstructural variations is beyond the scope of this study, a few trends can be determined from the results obtained for the 811 and 5621S alloys. As is evident from the threshold curves determined for the 811 alloy, microstructural changes can dramatically alter the alloy's susceptibility to stress-corrosion. For example, a microstructure which consists of a distribution of beta in a continuous matrix of primary alpha (fig. 8(a)), as a result of

mill annealing at temperatures low in the alpha plus beta phase field, was quite susceptible to stress-corrosion. Resistance to stress-corrosion could be substantially increased by annealing at temperatures higher in the alpha plus beta phase field. The microstructure then consists of a distribution of discontinuous, equiaxed islands of primary alpha in a continuous matrix of transformed beta (see fig. 8(d)).

These results are consistent with earlier investigations in both hot-salt (refs. 18 to 21) and salt water (refs. 22 to 24) environments. These studies demonstrated that a structure consisting of discontinuous primary alpha was more resistant to cracking than a matrix of continuous primary alpha.

Annealing titanium alloys at still higher temperatures can adversely affect stress-corrosion resistance. For example, the results obtained for the 5621S alloy indicate that processing and/or annealing above the beta transus drastically decreases resistance to stress-corrosion. Specifically, when the 5621S (1) alloy was processed and annealed at temperature high in the alpha plus beta field, but below the beta transus, the resultant structure of discontinuous alpha in a continuous matrix of transformed beta (fig. 8(k)) was the most resistant condition tested in this investigation. Processing in the alpha plus beta field followed by beta annealing (2A) resulted in a transformed beta (Widmanstätten) microstructure (fig. 8(*l*)). This structure, which consists of narrow beta-rich platelets dispersed between elongated alpha grains, exhibited intermediate resistance to stress-corrosion. However, still poorer resistance was achieved when the 5621S alloy was processed and annealed entirely within the beta field or even reannealed in the alpha plus beta field. For example, the 5621S (2B) and (2C) conditions were the least resistant alloys tested in this program. The resultant structure, consisting of a matrix of acicular transformed beta with either silicides or beta phase at the prior beta grain boundaries (figs. 8(m) to (p)), is extremely sensitive to hot-salt stress-corrosion cracking.

Microstructure-resistant alloys. - The 679, 6242, and 64 alloys do not appear to be as sensitive to microstructural variations as are the 811 and 5621S alloys. For example, only minor differences in threshold curves were observed for these three alloys for the heat treatments used in this study. The 679, 6242, and 64 alloys were tested with microstructures that consisted of both continuous alpha and discontinuous alpha.

However, limited data reported by the General Electric Co. (private communication with C. E. Shamblen and H. M. Green) indicated that the threshold stress of one heat of 64 alloy mill annealed at 700° C (1300° F) for 2 hours, AC, could be decreased about 35 percent by annealing near or above the beta transus followed by aging treatments. The threshold stress of the same material could be increased about 50 percent by warm working at temperatures slightly above the mill annealing temperature.

The literature data discussed previously and the results obtained in this investiga-

tion for the 5621S alloy serve as examples of the dramatic influence of microstructural variations. Hence, caution should be exercised when interpreting the stress-corrosion resistance of the 679, 6242, and 64 alloys. It is possible that abusive processing and heat treating conditions could markedly degrade the excellent resistance to stress-corrosion observed in this investigation. It is also probable that other variables such as grain size and forging anisotropy could exert significant effects on an alloy's susceptibility to hot-salt stress-corrosion cracking.

Heat-to-heat variations. - Although the study of heat-to-heat variations was not a specific purpose of this investigation, limited data reported by the General Electric Co. (private communication with C. E. Shamblen and H. M. Green) demonstrate that heat-to-heat variations could drastically influence susceptibility to stress-corrosion cracking. For example, threshold data determined for 4 heats of the 64 mill annealed alloy exhibited substantial variations. The 200 hour crack threshold stress at 430° C (800° F) varied from about 140 to 280 MN/m^2 (20 to 40 ksi). Another investigation (ref. 18) demonstrated that heat-to-heat variations resulted in a 100 hour crack threshold stress range of from 90 to 160 MN/m^2 (13 to 23 ksi) for the 811 mill annealed alloy at an exposure temperature of 430° C (800° F). Heat-to-heat variations were reported by another investigator (ref. 25) as having significant effects on susceptibility to hot-salt stress-corrosion.

Cooling rate from mill anneal. - An additional variable was determined for the 811 alloy. The as-received alloy was tested in the mill annealed/air cooled condition. Some of the bar stock was reannealed under similar conditions followed by furnace cooling. Although no significant microstructural differences could be resolved, substantial differences in threshold curves were measured. It is probable that the furnace cooled condition contains the ordered structure (ref. 26) or coherent phase (ref. 27) Ti_3Al. Although X-ray confirmation was not attempted, several previous investigators have reported the occurrence of the phase after slow cooling through or prolonged annealing in the temperature range about 500° to 600° C (930° to 1110° F), particularly for alloys with high aluminum contents such as the 811 alloy (refs. 12, 14, and 15). The influence of cooling rate is also apparent from the excellent resistance to stress-corrosion exhibited by the 811 alloy in the duplex annealed condition. Even though the alloy was annealed for an extended period at 650° C (1200° F), air cooling apparently minimized or prevented the formation of Ti_3Al.

Effect of Surface Condition

The influence of specimen surface condition on susceptibility to hot-salt stress-corrosion was evaluated by determining threshold curves for many of the alloys with specimens in both the as-machined and chemically milled surface conditions. Crack

threshold curves determined in the dynamic air environment for 811 mill anneal/air cooled, 64 duplex, and 6242 mill anneal alloys are shown in figure 4. It is evident that the crack threshold curve exhibited by chemically milled specimens is substantially below the threshold curve exhibited by specimens in the as-machined condition. For at least one exposure temperature for each of these three alloys, the difference between the threshold stresses was 210 to 350 MN/m^2 (30 to 50 ksi). For most of the other alloys tested, the chemically milled threshold curve usually occurred at stresses up to 70 MN/m^2 (10 ksi) below the threshold curve exhibited by as-machined specimens.

As demonstrated by these results, specimen surface condition can exert a significant influence on susceptibility to hot-salt stress corrosion. The fact that most thresh-

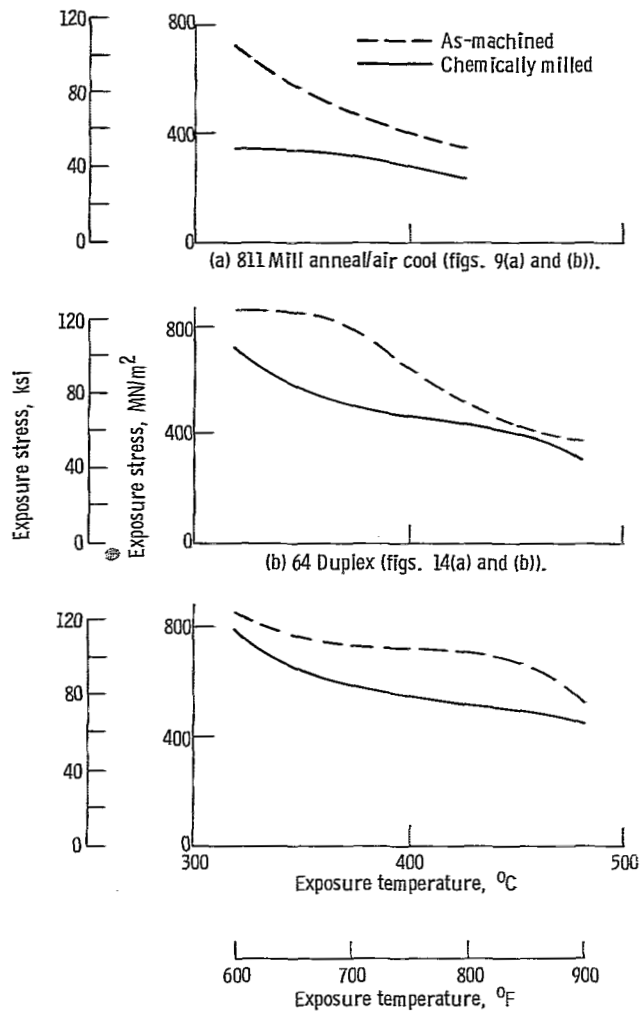

Figure 4. - Crack threshold curves for as-machined and chemically milled specimens of several alloys (dynamic air).

old curves occurred at lower stresses for chemically milled (stress-relieved) than for as-machined specimens suggests that the residual surface stresses resulting from machining the bore of the tubular specimens were compressive. A previous investigation (ref. 6) unsuccessfully attempted to use X-ray techniques to confirm both the magnitude and sign of the stress.

However, the assumption regarding the sign of the residual stress is consistent with the type of machining operation involved and with the results of another investigation (ref. 28) which demonstrated that mechanically induced (glass-bead peening and vibratory cleaning techniques) residual compressive stresses were effective in preventing or alleviating hot-salt stress-corrosion of the 811 alloy. Additional research by these investigators (ref. 29) has indicated that compressive stresses up to about 830 MN/m^2 (120 ksi) can result from glass bead peening. They studied the annealing kinetics of residual stresses for the 64 alloy. After 100 hours exposure at 320° C (600° F) about 75 percent of the original stress level remained. However, after a similar exposure at 430° C (800° F) only 25 percent of the residual compressive stress level remained. These results were independent of the type of peening and the initial magnitude of the residual surface stresses.

Results obtained for the 679 alloy showed that the 100 hour threshold stress at 430° C (800° F) increased from 150 MN/m^2 (22 ksi) to either 350 or 480 MN/m^2 (50 or 70 ksi) depending on the magnitude of the peening intensity (private communication with H. M. Green, General Electric Co.). However, even this high creep strength alloy exhibited stress relaxation and a significant reduction of the protective effect of the residual stresses when exposed at 480° C (900° F).

In summary, both the results of this investigation and those discussed from the literature indicate that specimen surface condition can exert a major influence on susceptibility to stress-corrosion. Residual compressive stresses resulting from either machining or shot-peening can protect titanium alloys from hot-salt stress-corrosion. However, it must be emphasized that this protective influence can anneal out during long time, elevated temperature exposures.

Effect of Air Velocity

The influence of air velocity on susceptibility to hot-salt stress-corrosion was evaluated by determining threshold curves for specimens exposed in both static air laboratory furnaces and in the dynamic air facility. Specimens in the chemically milled surface condition were tested in these two environments for the following alloys and heat treatments: 811 mill anneal/air cooled and triplex, 64 mill anneal and duplex, 6242 mill anneal, and 13-11-3 duplex.

As reported previously (refs. 6 and 9), air velocity exerted only a minor influence on susceptibility to stress-corrosion of the 811 mill anneal/air cooled alloy. In all cases, threshold curves determined in dynamic air occurred at similar or slightly greater stresses than did threshold curves in static air. A variation of 140 MN/m^2 (20 ksi) was determined between the embrittlement threshold stress in the two air environments at 320° C (600° F) and about 70 MN/m^2 (10 ksi) at 430° C (800° F). Variations of 70 MN/m^2 (10 ksi) or less were measured between crack threshold stresses over the same temperature range. These variations were considered minor and within the degree of accuracy that can be obtained with tests of this nature. Hence, it was concluded that there was only a minor beneficial effect of air velocity.

Similar results were obtained for the alloys studied in this investigation. Dynamic air threshold curves occurred at stress levels equal to or slightly greater than static air threshold curves. In the great majority of cases, both the embrittlement and crack threshold stresses for the two environments were within 70 MN/m^2 (10 ksi) or less. For the 811 triplex, 64 mill anneal and duplex, 6242 mill anneal, and 13-11-3 duplex alloys, there were only 5 exposure conditions out of a total of 30 where the variation between threshold stresses was 140 MN/m^2 (20 ksi). In no cases were any differences larger that this determined.

Threshold curves for the 679 mill anneal and duplex and 6242 duplex were determined for as-machined specimens in dynamic air and for chemically milled specimens in static air. Although the effect of air velocity could not be determined precisely because of the differences in specimens surface conditions, it appeared that there was no effect of air velocity. Specifically, 22 out of 24 exposure conditions were within 70 MN/m^2 (10 ksi) or less. The other two exposure conditions resulted in differences of 140 MN/m^2 (20 ksi).

Hence, it can be concluded from this investigation that there is only a minor effect of the 340 meter per second (1100 ft/sec) dynamic air environment. However, this effect is beneficial in that the threshold curve determined in the dynamic air environment usually occurred at slightly higher exposure stresses than did the threshold curve determined in static air. It is possible that higher air velocities and pressures or an impinging airflow might result in additional beneficial effects.

Relation Between Embrittlement and Crack Thresholds

As mentioned in the INTRODUCTION, there are many criteria that have been used to define an alloy's susceptibility to hot-salt stress-corrosion. A previous investigation by the author (ref. 5) defined three types of 100 hour thresholds for as-machined specimens of the 811 mill anneal/air cooled alloy exposed to a dynamic air environment. Specifically, at 430° C (800° F), embrittlement became apparent at an exposure stress

of less than 70 MN/m^2 (10 ksi) only if tensile testing was performed at a low, constant crosshead speed of 0.01 centimeter per minute (0.005 in./min). Stress-corrosion cracks were not observed during metallographic examination at ×1000 until the exposure stress exceeded about 350 MN/m^2 (50 ksi). Cracks could easily be observed by examining the fracture surface optically at ×30. They were always oxidized and corroded and were located at the origin of a distinct crescent shaped failure plane on the fracture surface. For example, a crack only 0.006 centimeter (0.003 in.) deep is readily

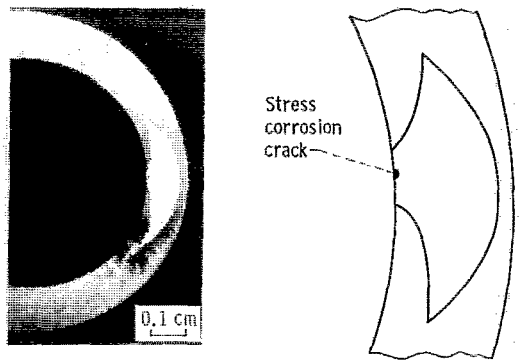

Figure 5. - Photomacrograph of hot-salt stress-corrosion crack.

apparent in figure 5. The lower limit of detectability by this technique is about 0.002 centimeter (0.001 in.). Brittle rupture occurred during exposure when the stress was about 580 MN/m^2 (85 ksi).

The sensitivity of this low-strain-rate testing procedure as a means of detecting the embrittlement threshold curve is also evident from data determined in this investigation. For instance, threshold curves for the 811 mill anneal/air cooled, 811 duplex, and 5621S (2A) alloys determined in dynamic air with chemically milled specimens are shown in figure 6. In all cases embrittlement threshold curves occurred at substantially lower exposure stresses than did crack threshold curves.

However, for the 64, 679, and 6242 alloys, the embrittlement threshold occurred at lower stresses than did the crack threshold curve for only a few of the exposure conditions tested. In those cases the embrittlement threshold stress was only about 70 MN/m^2 (10 ksi) less than the stress required for cracking. These alloys are so resistant to hot-salt stress-corrosion that they must be exposed near or above their creep strength to exhibit any damage. Hence, in many cases, the embrittlement and/or crack threshold stresses could not be determined because of creep limitations. Therefore, it is understandable that relative differences between the thresholds become obscured as the baseline approaches an imposed ceiling.

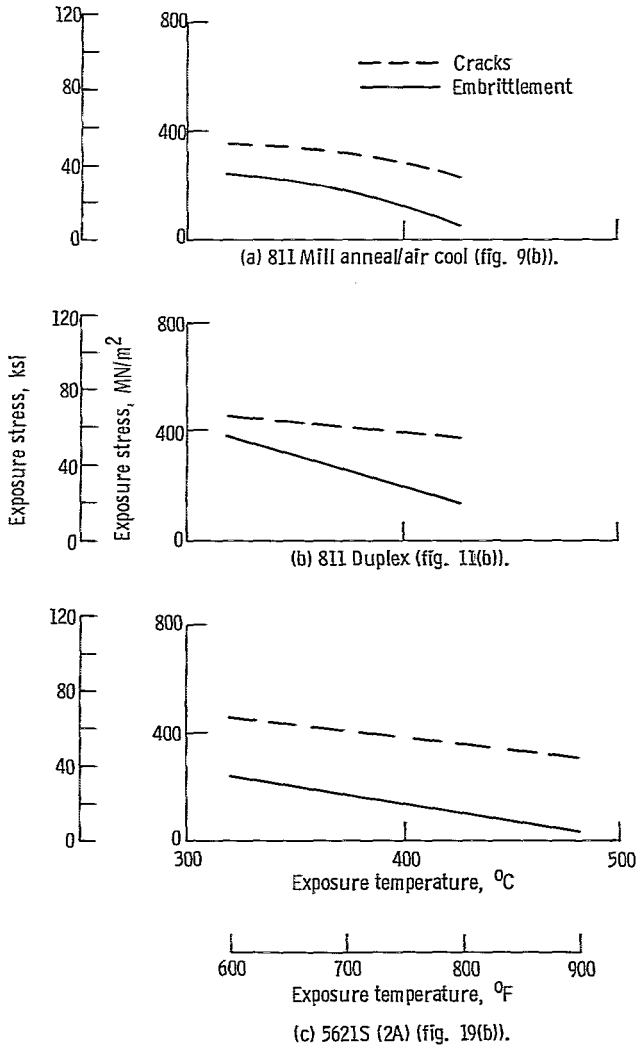

Figure 6. - Crack and embrittlement threshold curves for several alloys (chemically milled specimens, dynamic air).

It is also possible that the sensitivity of the embrittlement testing technique could be enhanced in these alloys under slightly different conditions of tensile strain rate and temperature. For example, maximum embrittlement was observed during low-strain-rate tensile testing at about 70° C (160° F) in the 6242 duplex alloy (private communication with H. M. Green, General Electric Co.) rather than at room temperature (ref. 4).

Effect of Exposure Time

As might be expected, crack threshold stresses for all alloys decreased as the exposure time at 480° C (900° F) was increased to 1000 hours (see fig. 7). However, the

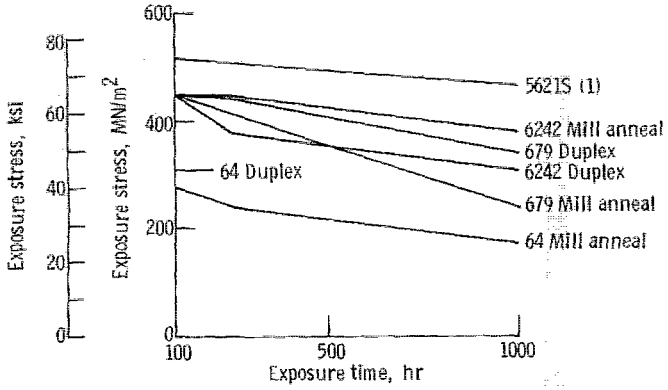

Figure 7. - Crack threshold curves for long-time exposures at 480° C (900° F) (chemically milled specimens, dynamic air). (See table XVIII.)

relative susceptibility of the alloys tested did not differ significantly from the 100 hour data discussed previously. The 5621S (1) alloy exhibited the best resistance to stress-corrosion and was followed by the 6242, 679, and 64 alloys.

Specifically, when the exposure time was increased from 100 to about 240 hours, either no changes or decreases of up to 70 MN/m^2 (10 ksi) were observed at 480° C (900° F) for all alloys. For exposure times of 1000 hours, a decrease in threshold stress of only 70 MN/m^2 (10 ksi) was observed for the 5621S (1) and 6242 mill anneal alloys. Decreases of up to 140 MN/m^2 (20 ksi) were observed for the other alloys except for the 679 mill anneal which exhibited a decrease in threshold stress of 210 MN/m^2 (30 ksi).

Cracks rather than embrittlement were used for defining these long-time threshold curves because of the possibility of embrittlement resulting from metallurgical instability masking embrittlement due to hot-salt stress-corrosion. However, although the data are not complete, it appears that the 5621S (1), 6242, 679, and 64 alloys are reasonably stable in the heat treated conditions used in this study. Of course, unsalted specimens should be exposed under similar conditions to accurately establish baseline ductility.

It should be noted that the salt contents measured on most of these specimens after stress-corrosion testing were somewhat below the intended, presalted concentrations. In all probability this loss of soluble chlorides can be attributed to chemical reactions occuring during the hot-salt stress-corrosion process.

Hydrogen Analyses

The author has previously reported (ref. 4) that increases in hydrogen content of stress-corroded titanium alloy specimens could be detected. Specifically, vacuum-fusion chemical analyses of 811 mill anneal/air cooled specimens that had been exposed to hot-salt stress-corrosion conditions indicated average hydrogen concentrations of from 100 to 255 ppm, as compared to the as-received alloy which contained about 70 ppm. Furthermore, a more recent investigation (ref. 5) demonstrated that this corrosion-produced hydrogen was concentrated below the salt-corroded and fracture surfaces of the specimens to concentration levels of several thousand ppm. It was also demonstrated that corrosion-produced hydrogen is responsible for embrittlement and cracking of the 811 titanium alloy subjected to hot-salt stress-corrosion exposures.

In addition, since these experiments demonstrated that hydrogen is highly segregated, the results of vacuum-fusion chemical analyses must be viewed with caution. This type of analysis represents only the total or average hydrogen concentration of the bulk sample submitted for analysis. It does not indicate the true concentration of hydrogen that may be segregated on a microscopic scale. In fact, unless the sample selected for analysis is small and taken close to the fracture surface, real increases in hydrogen content may be masked and indistinguishable from baseline values. In spite of these limitations, vacuum-fusion analyses are inexpensive and can yield valuable information. Consequently, hydrogen analyses were obtained for several stress-corrosion conditions of each of the alloys tested in this investigation. These results are presented in table IV.

As evident from these data, significant increases in hydrogen content of stress-corroded specimens were observed for all heat treatments of the alloys studied, with one exception. These analyses indicate that the hydrogen concentrations of these bulk samples were two to three times the level of the as-received alloy. The exception was the 13-11-3 alloy for which discrepancies between the vendor's and NASA's analyses of as-received bar stock could not be rationalized.

However, as discussed earlier, it must be emphasized that these bulk values of hydrogen reflect concentrations on a microscopic scale several orders of magnitude greater. Based on these results, corrosion-produced hydrogen appears to be involved in the embrittlement of all titanium alloys during hot-salt stress-corrosion. The techniques used to measure hydrogen concentration on a microscopic scale and the mechanism of hydrogen embrittlement have been discussed in detail in previous publications (refs. 3 to 5 and 8). This section is intended only to demonstrate the generality of the theory proposed earlier.

TABLE IV. - HYDROGEN ANALYSES OF AS-RECEIVED STOCK AND STRESS-CORRODED SPECIMENS

Alloy	Heat treatment	Bar stock or specimen[a]	Hydrogen concentration, ppm
811	Mill anneal/air cool	Stock	[b]70, [c]55 to 89
	Mill anneal/air cool	Refs. 4 and 5	100 to 255
	Mill anneal/furnace cool	323, 332, 321	91, 74, 78
	Triplex	200, 199, 170, 198	97, 104, 130, 126
64	Mill anneal	Stock	[b]50, [c]46 to 55
	Mill anneal	15, 36, 23	77, 84, 78
	Duplex	62, 66, 79	89, 73, 117
6242	Mill anneal	Stock	[b]70, [c]65 to 79
	Mill anneal	39, 33	132, 153
	Duplex	46, 61, 72	103, 108, 112
679	Mill anneal	Stock	[b]66, [c]58 to 88
	Mill anneal	31, 27	137, 109
	Duplex	61, 53	128, 118
5621S	2A	Stock	[b]36, [c]51 to 54
	2A	28, 39	63 to 67, 70 to 76
	2B	Stock	[b]36, [c]77 to 81
	2B	23	111, 120
	2C	Stock	[b]36, [c]133 to 157
	2C	14	171, 192
643	Duplex	Stock	[c]143, 152
	Duplex	1, 5	177, 207
13-11-3	Duplex	Stock	[b]104, [c]295 to 303
	Duplex	1, 24, 30, 18	269, 285, 302, 274

[a]See tables V to XVII for stress-corrosion exposure conditions.
[b]Vendor.
[c]NASA, usually ≥4 determinations.

CONCLUDING REMARKS

Microstructural and Processing Variables

The general trends apparent from the data of this investigation as well as the literature cited can be summarized as follows:

(1) A microstructure consisting of a discontinuous alpha phase in a transformed beta phase matrix (processing high in the alpha plus beta field) is most resistant to stress-corrosion.

(2) An acicular transformed beta structure (processing above the beta transus) is least resistant to stress-corrosion.

(3) A structure consisting of a continuous matrix of primary alpha (processing low in the alpha plus beta field) exhibits intermediate resistance to stress-corrosion.

(4) The Ti_3Al phase resulting from annealing in or slow cooling through a critical temperature range increases susceptibility to stress-corrosion for alloys containing more than about 6 percent aluminum.

Although nominal alloy composition and alloy partitioning between alpha and beta phases may play a significant role in determining alloy susceptibility to hot-salt stress-corrosion, it is felt that phase morphology is also of importance. The roles of both composition and structure in the process of stress-corrosion are undoubtedly complex. It is possible that the process of stress-corrosion cracking can be separated into at least three stages: (1) initial surface corrosion, (2) hydrogen absorption and diffusion, and (3) embrittlement and crack propagation. It is probable that the effects of both alloy and phase composition are most significant on the corrosion (refs. 11, 12, 23, and 25) and hydrogen absorption (refs. 14, 30, and 31) processes. Microstructure exerts an influence on both hydrogen embrittlement (refs. 32 and 33) and crack propagation or fracture toughness (refs. 12, 22 to 24, and 34). Obviously, additional research is needed to fully clarify and define all the critical steps involved in the process of hot-salt stress-corrosion of titanium alloys.

Variables Influencing Hot-Salt Stress-Corrosion

The results of this and previous investigations by the author (refs. 3 to 9) can now be summarized and used to answer one of the major questions that initiated this entire research program. Why have no documented service failures been reported for the titanium alloy compressor components that are operating under conditions of stress, temperature, and salt concentrations (refs. 3 and 7) which result in stress-corrosion failures in laboratory tests?

The major variables influencing stress-corrosion are as follows: (1) alloy composition, heat-to-heat variations, processing conditions; (2) specimen surface condition; and (3) cyclic exposure conditions.

Environmental variables such as air velocity, air pressure, air dewpoint, salt concentration, and salt deposition temperature exert only a minor influence on the susceptibility of the 811 alloy (refs. 6 and 9). The negligible influence of salt concentration was also spot checked in this investigation numerous times. Specimens of the 679, 6242, and 64 alloys were coated with 0.016 to 0.16 milligram per square centimeter (0.1 to 1 mg/in.^{2}), which was the concentration range frequently encountered in the compressors of jet engines (ref. 7). Almost invariably, salt concentrations in this range did not affect crack threshold stresses.

The major variables cited previously satisfactorily rationalize the reported lack of service failures. Specifically, most titanium alloy compressor components that are currently in service are made from the 64 alloy. This investigation has demonstrated that under simulated compressor environmental conditions the 64 alloy is creep limited and not stress-corrosion limited. In addition, most compressor components are shot-peened to produce residual compressive stresses on all surfaces. As this investigation has shown, substantially higher threshold stresses result for specimen surfaces with residual compressive stresses as compared to stress-free surfaces. Preliminary data from a current phase of the NASA hot-salt stress-corrosion program, together with several results in the literature (refs. 20, 28, and 35), also indicate that short cyclic exposures are not as severe as continuous exposures for equivalent total times. Since aircraft engines, especially military, operate for relatively short cycles, the 100 hour threshold curves commonly generated in laboratory investigations are representative of more severe conditions than the stress-temperature profiles of current titanium alloy compressor components.

However, there is still reason for concern that there may be service failures as developmental engines call for newer, stronger alloys that may be more susceptible to processing variables. These alloys are intended for use at higher operating stresses and temperatures and for longer cyclic periods. Under such operating conditions the beneficial effects of both cyclic exposures and shot-peening would be reduced.

SUMMARY OF RESULTS

The purpose of this investigation was to determine the relative susceptibility to hot-salt stress-corrosion of seven titanium alloys. The evaluation tests were conducted in a facility that simulated the environmental conditions encountered in the compressor of a jet-turbine engine. The alloys tested were 811, 64, 6242, 679, 5621S, 643, and 13-11-3. All but the 643 alloy are commercially available alloys, and they were usually

tested in two commonly used commercial heat treatments. Salt-coated specimens of these alloys were normally exposed for 100 hours in the temperature range 320° to 480° C (600° to 900° F). Specimens were then tensile tested at room temperature at a constant, low strain rate to determine residual ductility. When possible both embrittlement (less than 25 percent reduction of area and 15 percent elongation) and crack (corroded cracks on specimen fracture surface) threshold curves were determined.

1. Relative susceptibility to hot-salt stress-corrosion cracking can be drastically altered by heat-to-heat variations and processing conditions.

2. A comparison of standard 100 hour crack threshold curves indicates that susceptibility to hot-salt stress-corrosion increases in the following order: 679, 6242, 64, 643, 811, and 13-11-3. The 5621S alloy was both the least and most susceptible alloy depending on heat treatment.

3. When the alloys are compared on the basis of their potential use strength (100 hr crack threshold stress divided by stress for 0.2 percent creep in 100 hr), then the rankings are modified slightly: 64, 679, 6242, and 811. The 5621S alloy ranks either just above or below the 811 alloy, once again depending on the heat-treated condition of the 5621S alloy. Limited creep strength data for the 643 and 13-11-3 alloys precluded accurate rankings for these alloys.

4. The more resistant alloys, 679, 6242, and 64, exhibited only minor variations in threshold curves for the heat treatments tested. The more susceptible alloys, 811 and 5621S, exhibited substantial variations in threshold curves for the heat-treated conditions tested in this program. As mentioned previously, the 5621S alloy was both the least and most susceptible alloy tested in this program.

5. An alloy microstructure consisting of a discontinuous alpha phase in a transformed beta phase matrix appears to be most resistant to stress-corrosion. This structure can be achieved by working and/or annealing at temperatures high in the alpha plus beta phase field.

6. A microstructure consisting of a continuous matrix of primary alpha phase exhibits intermediate resistance to stress-corrosion. This structure results from working and annealing at temperatures low in the alpha plus beta phase field.

7. A microstructure consisting of acicular transformed beta phase is the structure that is least resistant to stress-corrosion. This structure can be achieved by working and/or annealing at temperatures above the beta transus.

8. An alloy heat treated under conditions likely to form Ti_3Al exhibits extreme sensitivity to stress-corrosion. This ordered phase results from slow cooling through or extended annealing in the temperature range 500° to 600° C (930° to 1110° F).

9. Residual surface compressive stresses resulting from specimen preparation reduce susceptibility to stress-corrosion. Specimens stress relieved by chemically milling the machined, compressively stressed surface exhibited a threshold curve at significantly lower stresses than did specimens in the as-machined condition. Major effects

were observed for the 811, 64, and 6242 alloys. Minor effects were observed for the 679 and 13-11-3 alloys. This variable was not determined for the 5621S and 643 alloys.

10. Only a minor reduction in susceptibility to stress-corrosion was observed in a dynamic air environment. The threshold curves for all alloys in the Mach 0.7 air environment generally did not exceed those in static air by more than 70 MN/m^2 (10 ksi).

11. The embrittlement threshold curve occurred at stress levels up to 350 MN/m^2 (50 ksi) lower than did the crack threshold curve for the more susceptible alloys, 811 and 5621S. For all other alloys, the embrittlement threshold curve was usually 70 MN/m^2 (10 ksi) lower than the crack threshold curve.

12. Increasing the stress-corrosion exposure time to 1000 hours resulted in decreases of from 15 to 50 percent in crack threshold stresses for all alloys tested. However, the relative susceptibility of the alloys remained essentially unchanged.

13. Increases in average bulk hydrogen content of from two to three times the as-received values were measured after several stress corrosion exposure conditions for each alloy tested in this program. These increases reflect concentrations on a microscopic scale as great as several thousand ppm. These chemical analyses support the concept that corrosion-produced hydrogen is responsible for hot-salt stress-corrosion embrittlement and cracking of titanium alloys.

Lewis Research Center,
National Aeronautics and Space Administration,
Cleveland, Ohio, July 2, 1971,
129-03.

REFERENCES

1. Anon.: Stress-Corrosion Cracking of Titanium. Spec. Tech. Publ. No. 397, ASTM, 1966.

2. Petersen, V. C.: Hot-Salt Stress-Corrosion of Titanium. J. Metals, vol. 23, no. 4, Apr. 1971, pp. 40-47.

3. Gray, Hugh R.: Hot-Salt Stress-Corrosion of Titanium Alloys. Aerospace Structural Materials. NASA SP-227, 1970, pp. 251-268.

4. Gray, H. R.: Hot Salt Stress Corrosion of a Titanium Alloy: Generation of Hydrogen and Its Embrittling Effect. Corrosion, vol. 25, no. 8, Aug. 1969, pp. 337-341.

5. Gray, Hugh R.: Role of Hydrogen in Hot-Salt Stress-Corrosion of a Titanium Alloy. NASA TN D-6188, 1971.

6. Gray, Hugh R.; and Johnston, James R.: Hot-Salt Stress-Corrosion of a Titanium Alloy in a Dynamic Air Environment. Metallurg. Trans., vol. 1, no. 11, Nov. 1970, pp. 3101-3105.

7. Ashbrook, Richard L.: A Survey of Salt Deposits in Compressors of Flight Gas Turbine Engines. NASA TN D-4999, 1969.

8. Gray, Hugh R.: Hot-Salt Stress-Corrosion of Titanium Alloys: Generation of Hydrogen and Its Embrittling Effect. NASA TN D-5000, 1969.

9. Gray, Hugh R.; and Johnston, James R.: Hot-Salt Stress-Corrosion of a Titanium Alloy Under a Simulated Turbine-Engine Compressor Environment. NASA TN D-5510, 1969.

10. Anon.: Quantab Chloride Titrators. Pamphlet 1104AD R636, Ames Co., Div. of Miles Laboratories, Inc., Elkhart, Ind., 1966.

11. Rideout, S. P.: The Initiation of Hot-Salt Stress Corrosion Cracking of Titanium Alloys. Applications Related Phenomena in Titanium Alloys. Spec. Tech. Publ. No. 432, ASTM, 1968, pp. 205-217.

12. Blackburn, M. J.; and Williams, J. C.: Metallurgical Aspects of the Stress Corrosion Cracking of Titanium Alloys. Conference on Fundamental Aspects of Stress Corrosion Cracking. Nat. Assoc. Corrosion Eng., 1969, pp. 620-637.

13. Seagle, S. R.; Seeley, R. R.; and Hall, G. S.: The Influence of Composition and Heat Treatment on the Aqueous-Stress Corrosion of Titanium. Applications Related Phenomena in Titanium Alloys. Spec. Tech. Publ. No. 432, ASTM, 1968, pp. 170-188.

14. Boyd, J. D.; Moreland, P. J.; Boyd, W. K.; Wood, R. A.; Williams, D. N.; and Jaffee, R. I.: The Effect of Composition on the Mechanism of Stress-Corrosion Cracking of Titanium Alloys in N_2O_4, and Aqueous and Hot-Salt Environments. NASA CR-1525, 1970.

15. Lane, I. R.; and Cavallaro, J. L.: Metallurgical and Mechanical Aspects of the Sea-Water Stress Corrosion of Titanium. Applications Related Phenomena in Titanium Alloys. Spec. Tech. Publ. No. 432, ASTM, 1968, pp. 147-169.

16. King, John A.: The Stress Corrosion Threat. Space/Aeronautics, vol. 46, no. 5, Oct. 1966, pp. 61-67.

17. Lane, I. R., Jr.; Cavallaro, J. L.; and Morton, A. G. S.: Sea-Water Embrittlement of Titanium. Stress-Corrosion Cracking of Titanium. Spec. Tech. Publ. No. 397, ASTM, 1966, pp. 246-259.

18. Danesi, W. P.; Sprague, R. A.; and Donachie, M. J., Jr.: The Effects of Microstructural Variations on Stress-Corrosion Cracking Susceptibility of Ti-8Al-1Mo-1V Alloy on Marinized Gas Turbines. Paper 67-GT-5, ASME, Mar. 1967.

19. Warmuth, Donald B.; and Kessler, Harold D.: How to Heat Treat Ti-8Al-1Mo-1V. Metal Prog., vol. 89, no. 3, Mar. 1966, pp. 91-94.

20. Piper, D. E.; and Fager, D. N.: The Relative Stress-Corrosion Susceptibility of Titanium Alloys in the Presence of Hot Salt. Stress-Corrosion Cracking of Titanium. Spec. Tech. Publ. No. 397, ASTM, 1966, pp. 31-52.

21. Simenz, R. F.; Van Orden, J. M.; and Wald, G. G.: Environmental Effects Studies on Selected Titanium Alloys. Stress-Corrosion Cracking of Titanium. *Spec. Tech. Publ.* No. 397, ASTM, 1966, pp. 53-79.

22. Curtis, R. E.; and Spurr, W. F.: Effect of Microstructure on the Fracture Properties of Titanium Alloys in Air and Salt Solution. Trans. ASM, vol. 61, no. 1, Mar. 1968, pp. 115-127.

23. Fager, D. N.; and Spurr, W. F.: Some Characteristics of Aqueous Stress-Corrosion in Titanium Alloys. Trans. ASM, vol. 61, no. 2, June 1968, pp. 283-292.

24. Hatch, A. J.; Rosenberg, H. W.; and Erbin, E. F.: Effects of Environment on Cracking in Titanium Alloys. Stress-Corrosion Cracking of Titanium. Spec. Tech. Publ. No. 397, ASTM, 1966, pp. 122-136.

25. Petersen, V. C.; and Bomberger, H. B.: The Mechanism of Salt Attack on Titanium Alloys. Stress-Corrosion Cracking of Titanium. Spec. Tech. Publ. No. 397, ASTM, 1966, pp. 80-94.

26. Blackburn, M. J.: Relationship of Microstructure to Some Mechanical Properties of Ti-8Al-1V-1Mo. Trans. ASM, vol. 59, no. 4, Dec. 1966, pp. 694-708.

27. Crossley, F. A.; and Carew, W. F.: Embrittlement of Ti-Al Alloys in the 6 to 10 Pct Al Range. J. Metals, vol. 9, no. 1, Jan. 1957, pp. 43-46.

28. Heimerl, G. J.; Braski, D. N.; Royster, D. M.; and Dexter, H. B.: Salt Stress Corrosion of Ti-8Al-1Mo-1V Alloy Sheet at Elevated Temperatures. Stress-Corrosion Cracking of Titanium. Spec. Tech. Publ. No. 397, ASTM, 1966, pp. 194-214.

29. Braski, David N.; and Royster, Dick M.: X-Ray Measurement of Residual Stresses in Titanium Alloy Sheet. Proceedings of the 15th Annual Conference on Applications of X-Ray Analysis. Vol. 10 of Advances in X-Ray Analysis. J. B. Newkirk and G. R. Mallett, eds., Plenum Press, 1967, pp. 295-310.

30. Sanderson, G.; and Scully, J. C.: Hydride Formation in Thin Foils of Dilute Ti-Al Alloys. Trans. AIME, vol. 239, no. 12, Dec. 1967, pp. 1883-1887.

31. Grushina, V. V.; Rodin, A. M.; Savitskiy, E. M.; and Burkhanov, G. S.: Hydrogen Absorption by Ti-Ni, Ti-Cr and Ti-Al Alloys. Russ. Metallurgy, no. 6, 1965, pp. 104-109.

32. Daniels, R. D.; Quigg, R. J.; and Troiano, A. R.: Delayed Failure and Hydrogen Embrittlement in Titanium. ASM Trans., vol. 51, 1959, pp. 843-861.

33. Kokhos, D. M.; and Seagle, S. R.: The Effect of Hydrogen on the Properties of Ti-6Al-4V. Rep. R&D 484, Reactive Metals, Inc., Feb. 1967.

34. Adams, R. E.; and von Tiesenhausen, E.: Study of Stress Corrosion Cracking of Commercial Titanium Alloys. Conference on Fundamental Aspects of Stress Corrosion Cracking. Nat. Assoc. Corrosion Eng., 1969, pp. 691-700.

35. Stone, L. H.; and Freedman, A. H.: Cyclic Hot-Salt Stress Corrosion of Titanium Alloys. Rep. NOR-67-151, Northrop Corp. (AFML-TR-67-289), Sept. 1967. (Available from DDC as AD-825239.)

TABLE V. - 811 MILL ANNEAL/AIR COOLED (FIGS. 9(a) TO (c))

Specimen	Exposure conditions						Tensile test data						Salt coating		Heat-tinted cracks
	Temperature		Time, hr	Stress		Creep, percent reduction of area	Ultimate stress		Fracture stress		Reduction of area, percent	Elongation, percent	mg/cm^2	$mg/in.^2$	
	°C	°F		MN/m^2	ksi		MN/m^2	ksi	MN/m^2	ksi					
As-machined, dynamic air (refs. 6 and 9)															
72	320	600	96	550	80	---	1030	150	940	136	32	18	0.02	0.13	No
[a]225				550	80	---	1010	147	910	132	32	19	.04	.24	
[a]226				620	90	---	1030	149	960	139	30	17	.06	.41	
53				620	90	---	1070	155	1070	155	11	10	.03	.17	
[a]253				690	100	---	1030	150	1030	150	10	8	.04	.28	
116			93	760	110	1.7	1040	151	1030	150	6	3	.10	.66	Yes
43	370	700	95	350	50	---	1030	149	900	131	35	18	.02	.13	No
[a]242			96	350	50	---	1040	151	940	137	30	19	.08	.53	
[a]247				410	60	---	1030	149	950	138	28	19	.06	.38	
70				410	60	---	1060	153	1060	153	14	9	.03	.20	
[a]248				480	70	---	1030	149	1030	149	16	10	.04	.23	
99			93	480	70	---	990	143	990	143	8	0	.08	.50	Yes
[a]239	430	800	96	70	10	---	1030	150	990	144	27	17	.06	.41	No
30				70	10	---	1050	152	1030	150	19	14	.03	.16	
[a]231				140	20	---	1030	149	960	139	27	18	.03	.17	
36				140	20	---	1020	148	1010	146	19	14	.04	.23	
[a]234				210	30	---	1060	153	1060	153	11	7	.07	.42	
18				350	50	---	1050	152	1050	152	10	8	.01	.09	
12			112			---	1040	151	1030	150	7	6	.03	.17	
107			92			---	1050	152	1050	152	4	3	.06	.41	
111			96			---	1060	153	1060	153	16	8	.07	.44	Yes
97			93	410	60	.3	1000	145	1000	145	7	3	.08	.51	Yes
Chemically milled, dynamic air (refs. 6 and 9)															
135	320	600	96	210	30	---	1010	146	930	135	30	18	0.08	0.53	No
289				210	30	---	1000	145	920	134	30	18	.07	.47	
[b]292				210	30	---	1010	147	920	134	32	20	.04	.26	
[c]296				280	40	---	1040	151	1040	151	12	10	.08	.54	
[d]303				280	40	---	1020	148	1010	147	16	10	.06	.42	
[e]304			94	280	40	---	1010	147	1010	147	12	9	.06	.41	
293			95	350	50	---	990	144	990	144	9	5	.09	.60	
128			96	350	50	---	990	143	990	143	5	7	.02	.15	Yes
311	370	700	96	140	20	---	1010	147	920	134	30	16	.13	.81	No
281				210	30	---	1020	148	960	139	24	14	.05	.35	No
288				280	40	---	1020	148	1020	148	17	11	.06	.38	No
285				350	50	---	1010	147	1010	147	12	8	.08	.54	Yes
299	430	800	95	70	10	---	1030	149	1010	147	19	14	.08	.53	No
290	430	800	96	210	30	---	1020	148	1020	148	13	13	.06	.41	No
316	430	800	96	280	40	---	970	140	970	140	8	2	.06	.41	Yes
Chemically milled, static air															
284	320	600	96	210	30	---	1010	146	900	130	34	19	0.07	0.46	No
313				210	30	---	1010	147	900	131	34	19	.08	.53	
336				280	40	---	1020	148	920	133	33	18	.15	.97	
373				350	50	---	1030	150	900	131	34	20	.11	.73	
388				350	50	---	1010	147	910	132	34	18	.15	.94	
476				350	50	---	1030	150	920	134	34	20	.20	1.3	
443				380	55	---	1000	145	1000	145	10	5	.12	.80	Yes
385				410	60	---	790	115	790	115	4	1	.15	.99	Yes
337	430	800	96	70	10	---	1060	153	960	139	33	18	.14	.90	No
375				140	20	---	1060	153	1060	153	13	8	.15	.97	No
363				210	30	---	1050	152	1050	152	7	7	.09	.58	Yes
384				210	30	---	830	120	830	120	3	0	.15	.99	Yes

[a] *Tested 1 year after initial tests.*
[b] *Chemically milled, 0.005 cm (0.002 in.).*
[c] *Chemically milled, 0.001 cm (0.0005 in.).*
[d] Exposed at room temperature for 4 wk.
[e] Exposed at 200° C (400° F) for 2 hr.

All *other specimens tested soon after chemically milling, 0.002 cm (0.001 in.).*

TABLE VI. - 811 MILL ANNEAL/FURNACE COOLED (FIG. 10)

Specimen	Exposure conditions						Tensile test data						Salt coating		Heat-tinted cracks
	Temperature		Time, hr	Stress		Creep, percent reduction of area	Ultimate stress		Fracture stress		Reduction of area, percent	Elongation, percent	mg/cm^2	$mg/in.^2$	
	°C	°F		MN/m^2	ksi		MN/m^2	ksi	MN/m^2	ksi					
As-machined, dynamic air															
324	320	600	96	550	80	---	1010	147	940	136	32	23	0.04	0.26	No
326	320	600	96	550	80	---	1050	152	1020	148	25	20	.06	.37	No
332	320	600	96	620	90	---	1020	148	1020	148	9	11	.08	.54	Yes
325	370	700	95	280	40	---	1010	146	960	139	34	25	.13	.82	No
329	370	700	96	350	50	---	990	144	990	144	16	13	.07	.46	No
321	430	800	97	70	10	---	950	138	950	138	10	6	.11	.68	No
331	430	800	95	140	20	---	980	142	980	142	11	5	.03	.19	Yes
Chemically milled, dynamic air															
330	320	600	96	70	10	---	990	143	990	143	8	7	0.06	0.38	No
327	320	600	95	140	20	---	990	143	990	143	12	8	.02	.12	No
323	320	600	96	210	30	---	970	140	970	140	5	1	.05	.33	Yes

TABLE VII. - 811 DUPLEX (FIGS. 11(a) AND (b))

Specimen	Exposure conditions						Tensile test data						Salt coating		Heat-tinted cracks
	Temperature		Time, hr	Stress		Creep, percent reduction of area	Ultimate stress		Fracture stress		Reduction of area, percent	Elongation, percent	mg/cm^2	$mg/in.^2$	
	°C	°F		MN/m^2	ksi		MN/m^2	ksi	MN/m^2	ksi					
As-machined, dynamic air															
424	320	600	94	620	90	---	1060	153	990	144	27	17	0.08	0.52	No
423	320	600	96	760	110	0.9	1030	150	1030	150	5	1	.12	.78	Yes
273	430	800	95	280	40	---	1070	155	970	140	34	20	.08	.49	No
276	↓	↓	96	410	60	---	1080	156	1010	146	30	19	.08	.52	↓
426			95	410	60	---	1080	157	1020	148	28	16	.14	.91	
274			94	480	70	1.2	1100	160	1030	149	30	18	.02	.14	
429			97	480	70	.7	1070	155	1070	155	13	8	.09	.56	↓
422	↓	↓	95	550	80	1.5	1060	154	1060	154	8	5	.05	.29	Yes
Chemically milled, dynamic air															
277	320	600	94	70	10	---	1080	156	970	141	33	20	0.05	0.30	No
275	↓	↓	95	210	30	---	1080	156	970	141	34	20	.07	.48	↓
278			94	350	50	---	1070	155	950	138	34	22	.12	.80	
428			96	410	60	---	1060	154	1060	154	16	11	.13	.85	↓
431	↓	↓	96	480	70	---	1020	148	1020	148	7	2	.17	1.1	Yes
425	430	800	94	210	30	---	1060	153	1060	153	13	9	.13	.87	No
430	430	800	96	280	40	---	1060	154	1060	154	13	8	.07	.42	No
427	430	800	97	350	50	0.2	1060	154	1060	154	11	9	.10	.66	No

TABLE VIII. - 811 TRIPLEX (FIGS. 12(a) TO (c))

Specimen	Exposure conditions						Tensile test data						Salt coating		Heat-tinted cracks
	Temperature		Time, hr	Stress		Creep, percent reduction of area	Ultimate stress		Fracture stress		Reduction of area, percent	Elongation, percent	mg/cm^2	$mg/in.^2$	
	°C	°F		MN/m^2	ksi		MN/m^2	ksi	MN/m^2	ksi					
As-machined, dynamic air															
177	320	600	96	690	100	0.6	950	138	860	125	35	20	0.05	0.32	No
[a]179	320	600	.1	760	110	41	----	---	----	---	41	23	.08	.50	↓
[a]191	320	600	.1	760	110	42	----	---	----	---	42	30	.15	.94	↓
194	370	700	96	410	60	.6	960	139	920	133	35	23	.06	.38	↓
181	370	700	95	480	70	----	960	139	940	137	23	17	.13	.86	↓
200	370	700	96	550	80	3.2	950	138	950	138	15	10	.10	.66	Yes
173	430	800	96	140	20	----	960	139	---	---	30	22	.09	.58	No
182	↓	↓	96	280	40	----	960	139	880	128	33	23	.06	.40	↓
196	↓	↓	95	350	50	----	950	138	890	129	32	24	.05	.35	↓
165	↓	↓	96	410	60	----	950	138	870	126	35	23	.03	.21	↓
[b]184	↓	↓	95	480	70	10	----	---	----	---	10	4	.05	.33	Yes
Chemically milled, dynamic air															
180	320	600	96	480	70	----	950	138	920	133	24	23	0.02	0.10	No
190	↓	↓	97	550	80	----	940	137	920	133	28	20	.07	.47	↓
183	↓	↓	97	550	80	----	940	136	940	136	13	10	.06	.41	↓
162	↓	↓	96	620	90	1.0	990	143	970	141	18	14	.08	.51	↓
161	↓	↓	96	690	100	7.7	1100	160	1080	157	8	2	.06	.37	Yes
166	370	700	96	280	40	----	950	138	920	134	24	20	.04	.26	No
186	↓	↓	96	350	50	----	960	139	960	139	17	12	.14	.87	Yes
172	↓	↓	94	410	60	----	940	137	900	130	33	21	.06	.37	No
176	↓	↓	96	410	60	.3	960	139	940	137	13	10	.14	.87	Yes
185	↓	↓	96	480	70	0	900	130	900	130	9	2	.07	.48	Yes
163	430	800	96	210	30	----	970	141	890	129	36	24	.01	.07	No
168	↓	↓	96	210	30	----	970	140	900	131	33	22	.06	.41	↓
182	↓	↓	98	280	40	----	960	139	950	138	18	14	.01	.03	↓
195	↓	↓	96	350	50	----	960	139	880	127	36	24	.06	.40	↓
188	↓	↓	96	350	50	----	940	136	930	135	19	10	.09	.55	Yes
170	↓	↓	96	410	60	0	951	138	950	138	17	11	.08	.49	Yes
Chemically milled, static air															
174	320	600	96	350	50	----	940	137	880	127	38	25	0.05	0.32	No
171	↓	↓	96	410	60	----	970	140	900	130	34	23	.10	.66	No
199	↓	↓	96	480	70	----	970	140	900	130	30	28	.02	.14	No
192	↓	↓	95	550	80	----	920	134	910	132	16	11	.14	.87	Yes
167	430	800	96	140	20	----	970	140	920	133	29	22	.08	.52	No
189	↓	↓	96	210	30	----	950	138	840	122	43	27	.02	.13	↓
193	↓	↓	97	280	40	----	960	139	920	134	29	23	.09	.60	↓
164	↓	↓	96	350	50	0	950	138	850	123	42	27	.03	.20	↓
178	↓	↓	97	350	50	0	950	138	940	137	21	14	.04	.25	↓
198	↓	↓	96	410	60	.6	790	115	790	115	6	2	.16	1.0	Yes

[a]Failed on loading.

[b]Failed during exposure.

TABLE IX. - 64 MILL ANNEAL (FIGS. 13(a) TO (c))

Specimen	Exposure conditions						Tensile test data						Salt coating		Heat-tinted cracks
	Temperature		Time, hr	Stress		Creep, percent reduction of area	Ultimate stress		Fracture stress		Reduction of area, percent	Elongation, percent	mg/cm^2	$mg/in.^2$	
	°C	°F		MN/m^2	ksi		MN/m^2	ksi	MN/m^2	ksi					
As-machined, dynamic air															
21	320	600	96	550	80	0.6	1090	158	950	138	33	16	0.17	1.0	No
37	↓	↓	↓	690	100	.3	1060	154	920	133	34	16	.01	.05	↓
32				760	110	3.0	1070	169	1030	150	29	12	.15	.96	
3				830	120	9.0	1390	202	1260	182	19	7	.15	.95	
4	370	700	95	550	80	0	1100	160	970	140	34	17	.14	.88	
11	370	700	95	620	90	2.0	1130	164	1010	147	28	15	.06	.39	↓
18	370	700	94	690	100	4.8	1170	170	1170	170	5	2	.08	.54	Yes
16	430	800	96	210	30	.7	1090	158	970	140	31	17	.01	.03	No
34	↓	↓	↓	280	40	.3	1100	160	960	139	33	17	.01	.03	↓
30				350	50	.7	1100	160	970	140	33	17	.12	.78	
6				410	60	.3	1090	158	940	136	34	18	.13	.85	
36				480	70	6.3	1200	174	1200	174	7	6	.08	.53	Yes
14	480	900	96	210	30	3.5	1150	167	1020	148	33	16	.03	.18	No
23	480	900	95	280	40	7.9	1260	183	1260	183	7	6	.06	.39	Yes
Chemically milled, dynamic air															
7	320	600	95	760	110	2.7	1170	169	1010	146	33	15	0.16	1.0	No
[a]28	320	600	.2	830	120	40	----	---	----	---	40	20	.09	.55	↓
12	370	700	96	550	80	.5	1100	160	940	137	36	17	.06	.38	
33	370	700	96	620	90	1.4	1130	164	990	143	31	15	.02	.14	↓
13	370	700	98	620	90	2.2	1120	163	1060	153	22	13	.02	.15	Yes
10	430	800	95	350	50	1.4	1150	167	1000	145	34	17	.11	.69	No
20	430	800	95	410	60	2.4	1130	164	1130	164	12	6	.15	.94	Yes
22	480	900	94	280	40	5.0	1170	169	1020	148	32	17	.09	.55	No
Chemically milled, static air															
17	320	600	96	690	100	0.6	1100	159	960	139	33	15	0.15	0.95	No
24	320	600	96	760	110	2.2	1150	166	1010	147	30	17	.14	.89	No
9	320	600	98	830	120	4.7	1280	186	1180	171	22	9	.15	.95	Yes
8	370	700	95	410	60	0	1100	159	940	136	36	18	.15	.95	No
[b]5	370	700	96	480	70	1.7	1120	162	1010	146	30	16	.22	1.4	No
27	370	700	96	550	80	.2	1100	159	1020	148	24	14	.14	.90	Yes
2	430	800	96	210	30	.6	1130	164	950	138	36	17	.14	.90	No
15	430	800	95	280	40	.5	1060	154	1060	154	10	3	.09	.58	Yes
25	480	900	94	140	20	1.7	1120	163	970	140	35	18	.07	.46	No
26	↓	↓	96	210	30	2.2	1130	164	980	142	35	18	.05	.31	↓
31			96	210	30	2.4	1140	165	970	140	36	18	.14	.91	
1			99	280	40	5.1	1190	172	1050	152	30	16	.14	.88	
40			96	280	40	5.0	1150	167	1150	167	10	3	.15	.97	Yes

[a]Failed on loading.

[b]Heavy salt.

TABLE X. - 64 DUPLEX (FIGS. 14(a) TO (c))

Specimen	Exposure conditions						Tensile test data						Salt coating		Heat-tinted cracks
	Temperature		Time, hr	Stress		Creep, percent reduction of area	Ultimate stress		Fracture stress		Reduction of area, percent	Elongation, percent	mg/cm^2	$mg/in.^2$	
	°C	°F		MN/m^2	ksi		MN/m^2	ksi	MN/m^2	ksi					
As-machined, dynamic air															
65	320	600	95	550	80	0	1170	170	1060	154	27	14	0.10	0.62	No
57	↓	↓	93	620	90	0	1190	173	1060	154	29	12	.15	.97	↓
58			95	690	100	.7	1180	171	1070	155	27	11	.12	.79	
60			96	760	110	.6	1180	171	1040	151	31	12	.17	1.1	
74			97	830	120	2.0	1250	181	1100	159	28	10	.14	.91	
48	370	700	96	620	90	1.2	1200	174	1090	158	25	11	.08	.53	
71	370	700	95	690	100	1.1	1190	172	1070	155	26	12	.15	.97	
43	370	700	96	760	110	1.5	1220	177	1100	159	26	9	.13	.87	
80	430	800	97	280	40	.4	1180	171	1060	153	29	15	.07	.48	
61	↓	↓	96	350	50	.7	1140	173	1080	156	28	14	.12	.80	
[a]59			70	410	60	2.7	1210	176	1070	155	31	14	.13	.81	
75			95	480	70	.6	1190	172	1060	154	31	15	.11	.69	↓
66			96	550	80	11.3	1150	167	1150	167	0	0	.12	.76	Yes
76	480	900	96	350	50	9.0	1300	189	1300	189	30	13	.04	.27	No
Chemically milled, dynamic air															
52	320	600	96	690	100	0.2	1170	169	1030	149	30	13	0.14	0.93	No
78	320	600	95	760	110	.5	1200	174	1110	161	22	12	.15	.99	Yes
50	370	700	96	480	70	0	1150	169	1000	145	34	16	.13	.83	No
47	↓	↓	97	550	80	.8	1190	172	1150	167	17	10	.11	.68	Yes
41			96	620	90	.5	1170	169	1120	163	17	8	.05	.35	Yes
56			97	690	100	.8	1190	173	1150	166	18	8	.06	.38	Yes
49	430	800	95	410	60	.2	1210	175	1040	151	32	13	.03	.21	No
72	430	800	96	480	70	1.6	1150	169	1150	169	3	0	.09	.59	Yes
63	480	900	95	280	40	1.9	1210	175	1080	157	29	12	.13	.81	No
51	480	900	96	350	50	5.1	1190	173	1190	173	8	2	.14	.91	Yes
Chemically milled, static air															
73	320	600	96	690	100	0	1150	167	990	144	33	14	0.12	0.77	No
64	320	600	96	760	110	.9	1200	174	1100	160	24	11	.15	.97	No
67	320	600	97	830	120	3.3	1250	182	1150	166	18	5	.25	1.6	Yes
69	370	700	95	550	80	.3	1170	170	1030	149	30	14	.09	.56	No
42	370	700	96	620	90	.3	1120	163	1070	155	19	11	.10	.63	Yes
45	430	800	96	280	40	0	1160	169	1020	148	32	14	.12	.76	No
46	430	800	96	350	50	.6	1130	172	1020	148	33	17	.14	.89	No
62	430	800	96	410	60	.9	1160	169	1160	169	7	1	.16	1.0	Yes
77	480	900	95	280	40	1.6	1190	172	1040	151	32	15	.10	.67	No
79	480	900	95	350	50	14	1250	182	1250	182	4	0	.07	.47	Yes

[a]Exposure terminated prematurely.

TABLE XI. - 6242 MILL ANNEAL (FIGS. 15(a) TO (c))

Specimen	Exposure conditions						Tensile test data						Salt coating		Heat-tinted cracks
	Temperature		Time, hr	Stress		Creep, percent reduction of area	Ultimate stress		Fracture stress		Reduction of area, percent	Elongation, percent	mg/cm^2	$mg/in.^2$	
	°C	°F		MN/m^2	ksi		MN/m^2	ksi	MN/m^2	ksi					
As-machined, dynamic air															
14	320	600	96	690	100	0	1060	154	940	136	31	18	0.14	0.89	No
26	320	600	96	760	110	0	1100	159	990	144	31	17	.07	.43	↓
9	320	600	96	830	120	1.6	1190	172	1050	152	29	11	.11	.71	
10	370	700	97	690	100	0	1110	161	1010	147	33	17	.10	.65	↓
18	370	700	96	760	110	.7	1090	158	1090	158	6	1	.16	1.0	Yes
8	430	800	97	410	60	0	1160	168	1030	149	31	16	.17	1.1	No
32	↓	↓	96	550	80	0	1120	162	980	142	31	17	.11	.69	↓
25			95	620	90	0	1150	167	1030	150	29	15	.12	.76	
21			96	620	90	---	1120	163	1030	150	29	15	.12	.80	
31			95	690	100	.6	1170	170	1030	149	31	16	.11	.68	↓
[a]23			16	760	110	9	----	---	----	---	9	7	.14	.87	Yes
22	480	900	95	210	30	---	1170	169	1030	150	30	18	.07	.42	No
29	↓	↓	96	410	60	.7	1150	167	1010	147	33	18	.14	.90	↓
15			↓	480	70	1.6	1150	167	1030	150	31	17	.02	.13	
12				480	70	1.0	1180	171	1060	153	30	15	.04	.24	
34				480	70	.6	1170	170	1020	148	33	10	.13	.84	↓
33	↓	↓	↓	550	80	3.4	1190	172	1190	172	15	8	.08	.49	Yes
Chemically milled, dynamic air															
84	320	600	96	760	110	1.9	1110	161	960	139	33	16	0.12	0.79	No
92	320	600	95	830	120	2.5	1210	175	1210	175	7	2	.12	.78	Yes
95	370	700	95	550	80	0	1090	158	1070	155	25	15	.09	.59	No
97	370	700	96	620	90	0	1100	159	1100	159	10	5	.14	.93	Yes
94	370	700	99	690	100	0	1090	158	1090	158	9	5	.10	.65	Yes
96	430	800	95	480	70	0	1100	159	960	139	33	16	.11	.68	No
81	430	800	99	550	80	.3	1070	155	1070	155	7	2	.17	1.1	Yes
91	430	800	94	620	90	.5	1120	162	1120	162	11	7	.12	.81	Yes
85	480	900	96	410	60	1.1	1150	166	990	143	36	17	.04	.24	No
98	480	900	96	480	70	1.5	1130	164	1120	163	12	10	.15	.98	Yes
Chemically milled, static air															
35	320	600	96	620	90	0	1140	165	980	142	35	17	0.15	0.98	No
7	320	600	96	690	100	0	1110	161	1040	151	24	13	.11	.68	No
5	320	600	96	760	110	---	1110	161	1110	161	12	7	.12	.80	Yes
4	370	700	95	550	80	0	1170	170	1080	156	26	14	.17	1.1	No
19	370	700	96	620	90	0	1120	163	1120	163	9	5	.12	.80	No
82	370	700	96	690	100	0	1100	159	1100	159	10	5	.14	.91	Yes
37	430	800	96	480	70	.3	1130	164	1010	146	31	16	.12	.81	No
40	430	800	96	550	80	---	1100	160	1100	160	10	8	.11	.74	Yes
[b]20	480	900	72	210	30	---	1150	167	----	---	27	16	.07	.47	No
2	↓	↓	94	280	40	.6	1150	167	1010	147	33	17	.10	.65	No
17			96	350	50	.6	1120	163	990	143	32	18	.10	.64	No
39	↓	↓	96	410	60	.5	1090	158	1090	158	6	3	.12	.77	Yes

[a]Failed during exposure.

[b]Exposure terminated prematurely.

TABLE XII. - 6242 DUPLEX (FIGS. 16(a) AND (b))

Specimen	Exposure conditions						Tensile test data						Salt coating		Heat-tinted cracks
	Temperature		Time, hr	Stress		Creep, percent reduction of area	Ultimate stress		Fracture stress		Reduction of area, percent	Elongation, percent	mg/cm^2	$mg/in.^2$	
	°C	°F		MN/m^2	ksi		MN/m^2	ksi	MN/m^2	ksi					
As-machined, dynamic air															
45	320	600	95	620	90	----	1030	150	930	135	33	20	0.09	0.59	No
76	320	600	97	690	100	0.5	1030	149	930	135	31	20	.07	.46	
56	320	600	94	760	110	4.0	1180	171	----	---	34	16	.10	.65	
44	370	700	96	480	70	----	1030	150	910	132	35	20	.13	.83	
73	↓	↓	95	550	80	----	1020	148	900	131	36	21	.08	.52	
48			96	620	90	----	1040	151	970	140	30	19	.07	.42	
64			96	690	100	1.2	1060	154	1060	154	8	9	.08	.49	Yes
52	430	800	94	410	60	----	1030	150	920	133	33	22	.07	.43	No
65			96	480	70	----	1060	154	940	137	33	21	.04	.26	
79			97	480	70	0	1030	150	930	135	35	21	.13	.84	
75			96	550	80	----	1030	150	960	139	30	21	.01	.04	
51			94	550	80	----	1030	150	920	134	34	21	.02	.11	
50			95	550	80	0	980	142	980	142	6	1	.15	.97	Yes
[a]61			30	620	90	9	----	---	----	---	9	2	.05	.31	Yes
62	480	900	94	410	60	----	1040	151	960	139	30	22	.02	.12	No
55			95	410	60	0	1050	152	920	134	35	21	.07	.47	No
53			94	480	70	1.6	1070	155	1070	155	13	10	.02	.14	No
46			96	550	80	3.5	1120	162	1100	160	13	11	.03	.21	Yes
Chemically milled, static air															
80	320	600	96	760	110	4.4	1170	169	1060	154	26	15	0.28	1.8	No
[b]49	320	600	.1	790	115	39	----	---	----	---	39	20	.14	.87	No
70	370	700	95	550	80	0	1030	150	940	137	32	18	.15	.97	No
77	370	700	96	620	90	2.7	1120	163	1080	156	23	14	.11	.72	Yes
74	430	800	96	350	50	----	1050	152	920	134	37	23	.03	.20	No
66			96	410	60	----	1030	149	930	135	35	22	.09	.55	No
[c]63			97	410	60	0	1050	152	1010	147	19	18	.16	1.0	No
78			96	480	70	----	960	139	930	135	21	10	.09	.58	Yes
42	480	900	96	350	50	----	1030	150	940	137	33	21	.06	.37	No
57			96	410	60	.3	1040	151	930	135	34	21	.05	.34	No
67			97	410	60	.6	1060	153	990	144	27	20	.10	.67	No
[a]72			29	480	70	10	----	---	----	---	10	5	.07	.45	Yes

[a]Failed during exposure.

[b]Failed on loading.

[c]Heavy salt plus chemically milled 0.005 cm (0.002 in.).

TABLE XIII. - 679 MILL ANNEAL (FIGS. 17(a) AND (b))

Specimen	Exposure conditions						Tensile test data						Salt coating		Heat-tinted cracks
	Temperature		Time, hr	Stress		Creep, percent reduction of area	Ultimate stress		Fracture stress		Reduction of area, percent	Elongation, percent	mg/cm^2	$mg/in.^2$	
	°C	°F		MN/m^2	ksi		MN/m^2	ksi	MN/m^2	ksi					
As-machined, dynamic air															
13	320	600	97	690	100	0.3	1070	155	940	137	33	19	0.12	0.78	No
9	320	600	97	760	110	3.3	1190	172	1080	156	14	12	.13	.82	No
5	370	700	96	620	90	0	1080	156	940	137	33	19	.11	.69	No
21	370	700	95	690	100	0	1060	154	1060	154	6	1	.15	.99	Yes
4	430	800	96	480	70	0	1040	151	940	136	32	20	.11	.71	No
12	↓	↓	98	550	80	0	1060	153	970	140	29	18	.01	.08	↓
8			93	550	80	0	1050	152	930	135	32	20	.10	.63	
2			95	550	80	0	1060	153	950	138	29	19	.11	.70	
[a]15			20	620	90	10	----	---	----	---	10	5	.20	1.3	Yes
10	480	900	97	350	50	----	1070	155	1000	145	27	19	.04	.27	No
22			96	410	60	0	1090	158	990	144	30	18	.01	.01	↓
19			↓	410	60	----	1060	154	990	144	31	19	.03	.21	
6				410	60	0	1060	153	1000	145	27	18	.05	.33	
31	↓	↓		480	70	0	1050	152	1050	152	9	5	.06	.41	Yes
Chemically milled, static air															
23	320	600	96	690	100	----	1040	151	910	132	33	17	0.15	0.97	No
25	320	600	96	760	110	2.7	1150	167	1030	150	28	14	.09	.59	↓
[b]24	320	600	.1	790	115	37	----	---	----	---	37	21	.13	.81	
36	370	700	96	550	80	0	1030	150	1010	146	22	15	.17	1.1	
30	370	700	95	620	90	1.2	970	141	970	141	4	2	.12	.76	Yes
20	430	800	96	480	70	.2	1060	153	980	142	29	18	.15	.99	No
39	430	800	95	550	80	.6	1040	151	1030	150	18	14	.11	.74	Yes
26	480	900	96	410	60	.6	1060	154	940	136	33	22	.01	.03	No
38	480	900	96	410	60	.6	1060	154	990	143	25	17	.11	.72	No
[c]27	480	900	72	480	70	18	1030	150	1010	146	18	14	.11	.68	Yes

[a]Failed during exposure.

[b]Failed on loading.

[c]Exposure termined prematurely.

TABLE XIV. - 679 DUPLEX (FIGS. 18(a) AND (b))

Specimen	Exposure conditions						Tensile test data						Salt coating		Heat-tinted cracks
	Temperature		Time, hr	Stress		Creep, percent reduction of area	Ultimate stress		Fracture stress		Reduction of area, percent	Elongation, percent	mg/cm^2	$mg/in.^2$	
	°C	°F		MN/m^2	ksi		MN/m^2	ksi	MN/m^2	ksi					
As-machined, dynamic air															
60	320	600	96	690	100	0.7	1090	158	1010	146	28	19	0.08	0.51	No
62	320	600	97	760	110	1.6	1150	166	1050	152	25	14	.11	.72	
69	320	600	95	790	115	2.2	1170	169	1050	152	24	13	.08	.53	
57	370	700	93	620	90	0	1080	156	980	142	27	17	.12	.76	
77	370	700	80	690	100	.4	1030	149	980	142	24	13	.11	.72	
[a]41	370	700	36	760	110	11	----	---	----	---	11	5	.15	.97	Yes
45	430	800	96	350	50	----	1040	151	970	140	29	19	.08	.49	No
51			96	480	70	----	1100	159	990	143	31	18	.05	.34	
75			96	550	80	----	1090	158	1000	145	27	18	.01	.02	
73			97	550	80	0	1090	158	1010	146	27	17	.13	.83	
70			95	620	90	.7	1080	156	990	144	33	18	.03	.20	
[a]50			87	620	90	8	----	---	----	---	8	4	.13	.86	Yes
[a]54			14	690	100	10	----	---	----	---	10	5	.08	.49	Yes
81	480	900	94	410	60	----	1090	158	970	140	33	20	.02	.13	No
74			95	480	70	----	1150	166	1010	147	27	18	.04	.25	No
64			96	550	80	.8	1100	160	1060	154	22	14	.03	.16	No
63			96	620	90	1.5	1110	161	1110	161	8	5	.03	.20	Yes
Chemically milled, static air															
55	320	600	96	690	100	1.0	1100	160	960	139	35	19	0.08	0.48	No
49	320	600	96	760	110	2.9	1170	170	1080	156	31	10	.12	.78	
[b]58	320	600	.1	830	120	38	----	---	----	---	38	23	.11	.69	
47	370	700	95	550	80	0	1080	156	1030	149	25	17	.09	.59	
56	370	700	95	620	90	3.3	1200	174	1120	162	22	9	.08	.53	
76	430	800	96	480	70	----	1060	154	950	138	32	19	.03	.19	
[c]78				480	70	----	1060	154	1000	145	26	18	.25	1.6	
[d]79				480	70	----	1070	155	1030	149	21	18	.12	.78	
[c]46				550	80	.6	1060	154	1060	154	12	10	.20	1.3	Yes
43			95	550	80	0	1090	158	1070	155	13	14	.04	.23	No
67			96	620	90	1.2	1100	160	1080	157	21	13	.02	.12	
48	480	900	96	410	60	0	1090	158	1000	145	28	17	.09	.60	
42				410	60	.6	1090	158	1020	148	27	15	.04	.28	
61				480	70	.6	1040	151	1040	151	6	3	.04	.29	Yes
68				550	80	1.2	1100	159	1100	159	8	7	.02	.10	Yes

[a]Failed during exposure.
[b]Failed on loading.
[c]Heavy salt.
[d]Chemically milled 0.005 cm (0.002 in.).

TABLE XV. - 5621S, CHEMICALLY MILLED, DYNAMIC AIR (FIGS. 19(a) TO (d))

Specimen	Exposure conditions						Tensile test data						Salt coating		Heat-tinted cracks
	Temperature		Time, hr	Stress		Creep, percent reduction of area	Ultimate stress		Fracture stress		Reduction of area, percent	Elongation, percent	mg/cm^2	$mg/in.^2$	
	°C	°F		MN/m^2	ksi		MN/m^2	ksi	MN/m^2	ksi					
Heat treatment (1)															
51	320	600	95	690	100	0	1080	157	1010	146	28	15	0.24	1.6	No
47	320	600	96	760	110	.5	1090	158	1030	149	23	10	.12	.80	Yes
50	480	900	93	350	50	0	1110	161	990	144	34	17	.11	.70	No
48	↓	↓	93	410	60	0	1100	159	990	143	33	16	.07	.49	No
44			95	480	70	0	1100	160	1060	153	27	13	.12	.77	No
52			95	550	80	.5	1110	161	1060	153	28	15	.12	.77	Yes
Heat treatment (2A)															
29	320	600	96	210	30	---	1100	160	1040	151	25	13	0.14	0.89	No
30	↓	↓	↓	280	40	---	1080	157	1080	157	7	5	.17	1.1	No
32				410	60	---	1090	158	1090	158	6	2	.14	.91	No
36				480	70	---	1100	159	1100	159	6	3	.02	.10	Yes
34				550	80	.3	1090	158	1090	158	5	3	.07	.48	Yes
26	480	900	96	70	10	---	1100	160	1100	160	8	6	.06	.39	No
27	↓	↓	↓	210	30	.3	1120	162	1120	162	11	6	.05	.33	↓
[a]38				280	40	0	1130	164	1080	157	25	13	----	----	
31				280	40	0	1090	158	1090	158	7	3	.07	.49	
39			95	350	50	.8	1060	154	1060	154	4	1	.07	.47	Yes
28			94	480	70	2.4	1060	153	1060	153	4	1	.11	.71	Yes
Heat treatment (2B)															
24	320	600	96	140	20	---	1070	155	1030	150	26	17	0.04	0.25	No
20	↓	↓	99	140	20	---	1080	156	1020	148	26	17	.09	.55	↓
18			96	210	30	---	1060	154	1040	151	20	15	.05	.33	
17			↓	280	40	---	1070	155	1070	155	8	6	.12	.82	
16				350	50	---	1030	150	1030	150	6	1	.19	1.2	Yes
19	↓	↓	↓	410	60	---	1020	148	1010	146	7	2	.04	.24	↓
22	480	900	95	70	10	---	1060	154	1060	154	6	2	.01	.01	
23	480	900	96	210	30	---	1020	148	1020	148	5	2	.12	.79	↓
Heat treatment (2C)															
[a]9	320	600	95	70	10	---	1090	158	1070	155	19	14	----	----	No
5	↓	↓	96	70	10	---	1020	148	1000	145	9	3	0.11	0.68	No
15			96	140	20	---	1010	147	1010	147	9	5	.09	.59	Yes
11			96	280	40	---	1000	145	940	137	7	3	.02	.11	Yes
[a]3	480	900	95	70	10	---	1100	159	1100	159	13	11	----	----	No
10	480	900	95	70	10	---	1040	151	1040	151	8	2	.13	.86	Yes
14	480	900	96	210	30	---	1010	147	1010	147	7	1	.06	.37	Yes

[a]Unsalted.

TABLE XVI. - 643 DUPLEX, CHEMICALLY MILLED, DYNAMIC AIR (FIG. 20)

Specimen	Exposure conditions						Tensile test data						Salt coating		Heat-tinted cracks
	Temperature		Time, hr	Stress		Creep, percent reduction of area	Ultimate stress		Fracture stress		Reduction of area, percent	Elongation, percent	mg/cm^2	$mg/in.^2$	
	°C	°F		MN/m^2	ksi		MN/m^2	ksi	MN/m^2	ksi					
3	320	600	97	550	80	---	1480	215	1480	215	4	1	0.08	0.52	No
7	320	600	96	620	90	---	1580	229	1580	229	5	1	.07	.46	No
8	320	600	95	690	100	0	1340	194	1340	194	2	1	.17	1.1	Yes
2	430	800	95	140	20	0.3	1580	229	1580	229	4	2	.05	.34	No
1	↓	↓	96	280	40	1.9	1610	234	1610	234	2	0	.05	.33	No
4			97	350	50	1.3	1580	229	1580	229	5	1	.12	.75	No
5			95	410	60	3.9	850	123	850	123	0	0	.03	.21	Yes

TABLE XVII. - 13-11-3 DUPLEX (FIGS. 21(a) TO (c))

Specimen	Exposure conditions						Tensile test data						Salt coating		Heat-tinted cracks
	Temperature		Time, hr	Stress		Creep, percent reduction of area	Ultimate stress		Fracture stress		Reduction of area, percent	Elongation, percent	mg/cm^2	$mg/in.^2$	
	°C	°F		MN/m^2	ksi		MN/m^2	ksi	MN/m^2	ksi					
As-machined, dynamic air															
[a]40	320	600	96	70	10	---	1070	155	1070	155	3	1	----	----	No
21	↓	↓	↓	280	40	---	1280	186	1280	186	7	5	0.07	0.44	No
10				350	50	---	1220	177	1220	177	5	2	.06	.39	Yes
20				410	60	---	1190	173	1190	173	3	1	.13	.83	Yes
18				480	70	0	1220	177	1220	177	3	1	.07	.44	Yes
35	430	800	95	280	40	0.7	830	121	830	121	0	0	----	----	No
9	430	800	96	350	50	.3	1090	158	1090	158	2	0	.02	.11	No
1	430	800	96	410	60	1.8	1400	203	1400	203	2	1	.01	.03	Yes
Chemically milled, dynamic air															
33	320	600	96	140	20	---	1170	170	1170	170	3	1	0.09	0.59	No
28	↓	↓	98	280	40	---	1100	159	1100	159	1	1	.04	.27	No
23			95	350	50	---	1320	191	1320	191	3	2	.13	.83	Yes
17			97	410	60	---	1080	157	1080	157	1	1	.07	.44	No
30			96	480	70	0	1260	182	1260	182	2	1	.09	.59	Yes
14	430	800	96	210	30	1.0	1160	168	1160	168	2	0	.05	.35	No
22	430	800	95	280	40	.9	1220	177	1220	177	2	1	.08	.52	No
24	430	800	97	350	50	.3	1340	195	1340	195	3	1	.03	.22	Yes
Chemically milled, static air															
4	320	600	97	210	30	---	1130	164	1130	164	2	1	0.13	0.85	No
38	320	600	96	280	40	---	1250	181	1250	181	5	4	.11	.73	Yes
11	430	800	97	140	20	0	1100	159	1100	159	1	1	.12	.79	No
12	430	800	96	210	30	0	1130	164	1130	164	1	1	.11	.68	No
34	430	800	96	280	40	1.2	1100	159	1100	159	3	1	.10	.66	Yes

[a]Unsalted.

TABLE XVIII. - INFLUENCE OF EXPOSURE TIME AT 480° C (900° F)

[Chemically milled, dynamic air (fig. 7).]

Specimen	Exposure conditions				Tensile test data						Salt coating		Heat-tinted cracks
	Time, hr	Stress		Creep, percent reduction of area	Ultimate stress		Fracture stress		Reduction of area, percent	Elongation, percent	mg/cm^2	$mg/in.^2$	
		MN/m^2	ksi		MN/m^2	ksi	MN/m^2	ksi					
64 Mill anneal													
39	235	210	30	9.9	1220	177	1050	152	34	14	0.11	0.72	No
29	1000	140	20	12	1270	184	1090	158	33	18	.03	.20	No
38	1000	140	20	17	1180	171	1080	156	28	11	.05	.29	No
[a]35	475	210	30	37	----	---	----	---	37	17	.03	.23	Yes
64 Duplex													
54	244	210	30	1.2	1180	171	1040	150	31	13	0.16	1.0	No
88	216	280	40	2.8	1230	178	1040	151	33	15	.03	.23	No
6242 Mill anneal													
87	242	420	60	1.5	1160	169	1050	152	32	14	0.04	0.27	No
93	1000	350	50	.8	1150	167	1070	155	28	15	.02	.16	↓
88	1005	350	50	1.3	1170	170	1080	156	30	14	.03	.20	↓
89	983	350	50	1.5	1190	173	1040	151	34	18	.04	.27	↓
83	1000	420	60	2.5	1180	171	1180	171	12	9	.04	.28	Yes
6242 Duplex													
54	216	280	40	0.6	1040	151	970	141	30	20	0.03	0.18	No
59	244	420	60	1.3	1060	153	1050	152	14	12	.02	.15	Yes
71	1000	280	40	0	1050	152	960	139	33	19	.04	.25	No
41	1000	350	50	.6	1050	152	1050	152	11	7	.03	.19	Yes
679 Mill anneal													
16	259	350	50	----	1060	153	990	143	28	16	0.05	0.30	No
37	240	350	50	0	1070	155	1020	148	24	15	.13	.84	No
17	240	420	60	.5	1070	155	1010	146	26	17	.04	.25	No
33	216	420	60	0	1020	148	1020	148	7	6	.17	1.1	Yes
14	1000	210	30	0	1060	154	1040	151	18	13	.03	.17	No
40	1001	210	30	0	1030	149	1020	148	18	14	.05	.31	No
35	1000	280	40	0	1050	152	1050	152	11	11	.05	.30	Yes
32	1000	350	50	.8	1060	154	1060	154	8	5	.01	.08	Yes
679 Duplex													
44	244	420	60	0	1080	157	990	144	27	16	0.10	0.67	No
80	216	480	70	.3	1090	158	1090	158	13	10	.12	.80	Yes
52	1000	280	40	0	1100	159	1060	153	23	15	.02	.13	No
5621S (1)													
43	1025	420	60	0	1120	163	1030	150	31	16	0.07	0.46	No
49	1004	480	70	.2	1120	163	1100	160	19	14	.05	.29	Yes

[a]Failed during exposure.

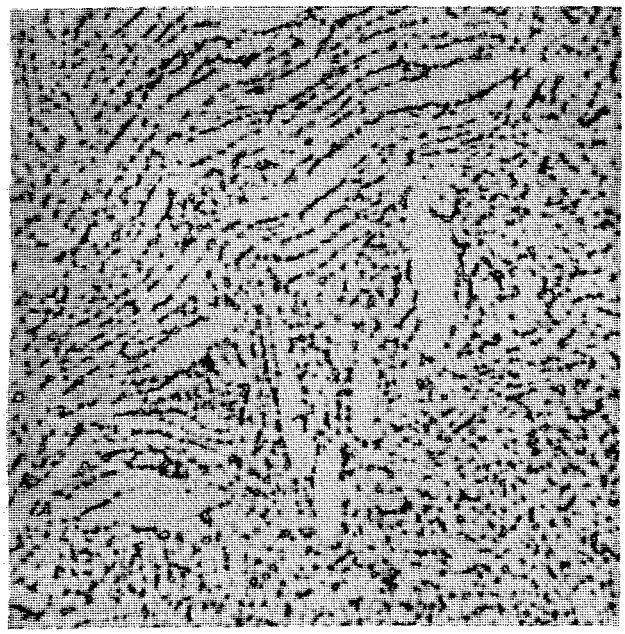

Transverse

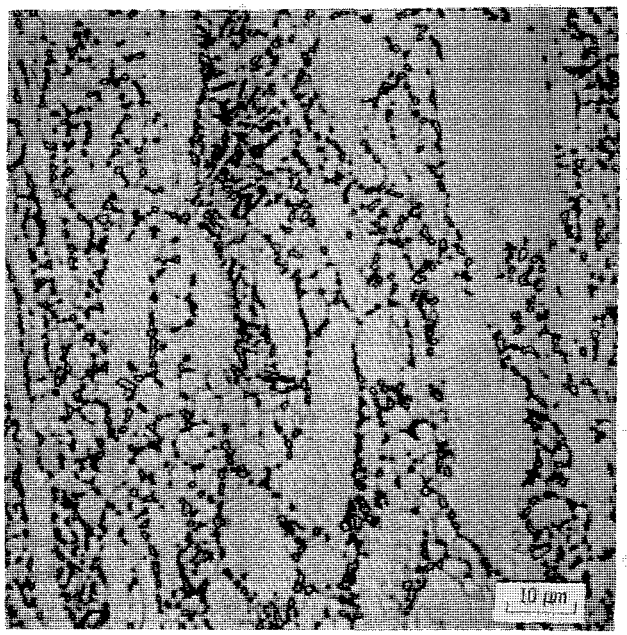

Longitudinal

(a) 811 Mill anneal/air cool.

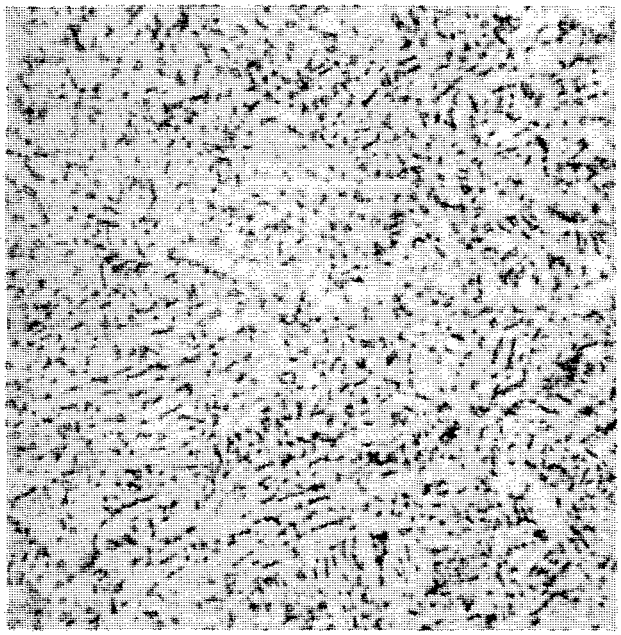

Transverse

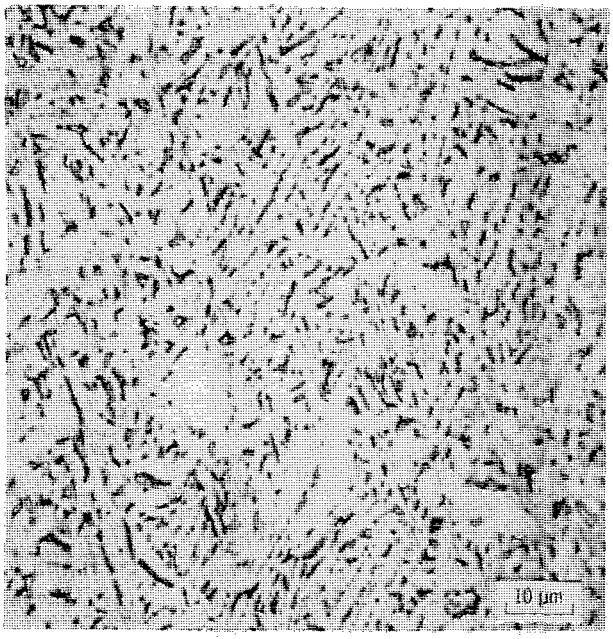

Longitudinal

(b) 811 Mill anneal/furnace cool.

Figure 8. - Photomicrographs of titanium alloys.

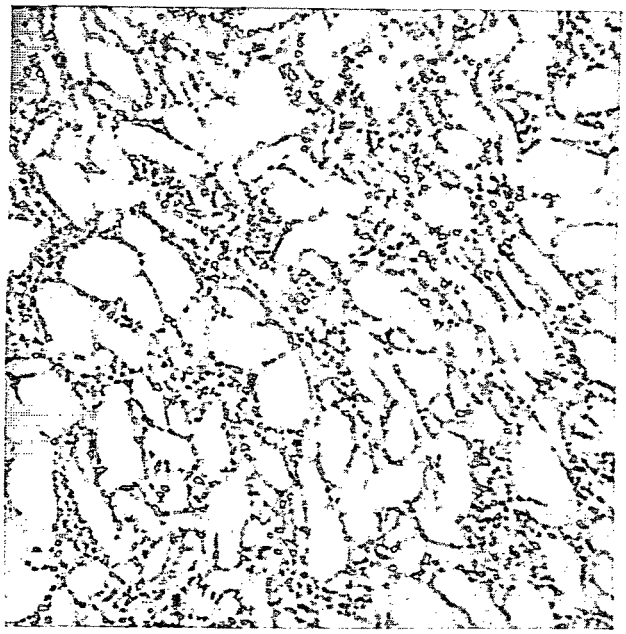

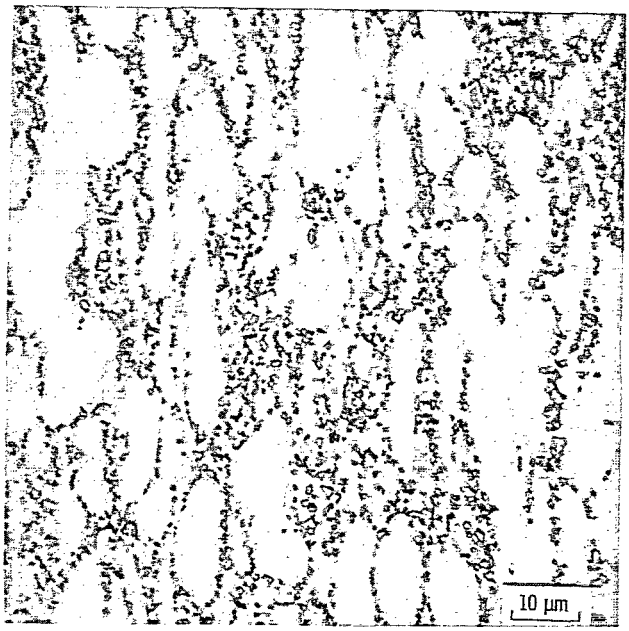

Transverse

Longitudinal

(c) 811 Duplex.

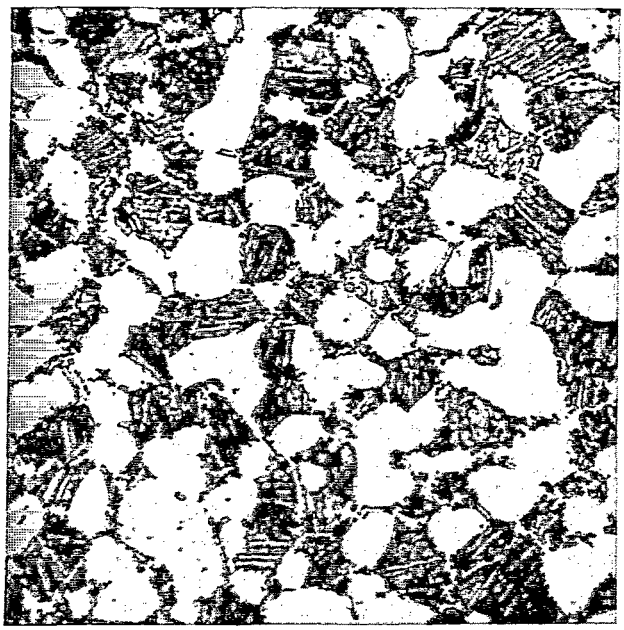

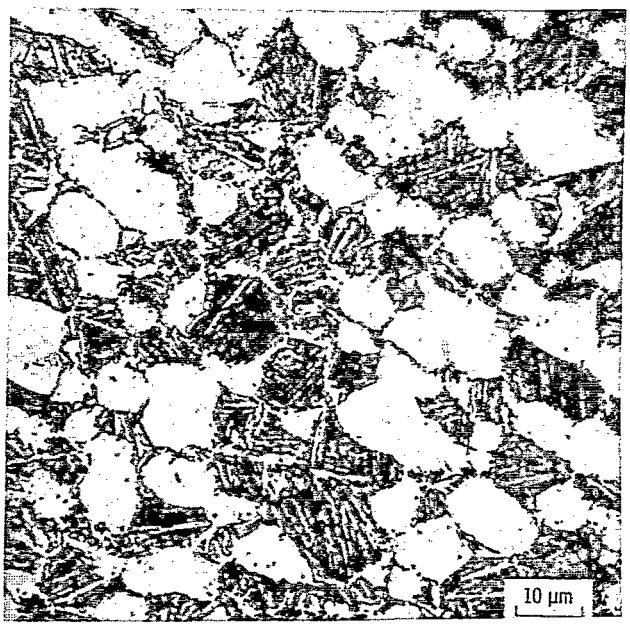

Transverse

Longitudinal

(d) 811 Triplex.

Figure 8. - Continued.

Transverse

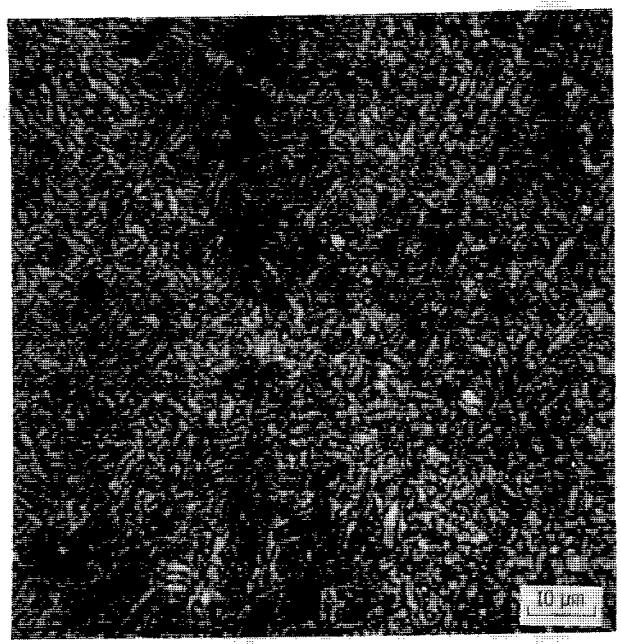

Longitudinal

(e) 64 Mill anneal.

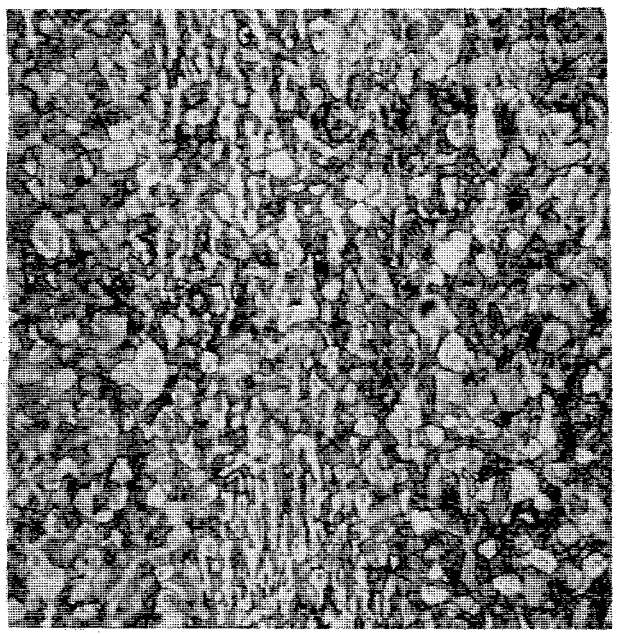

Transverse

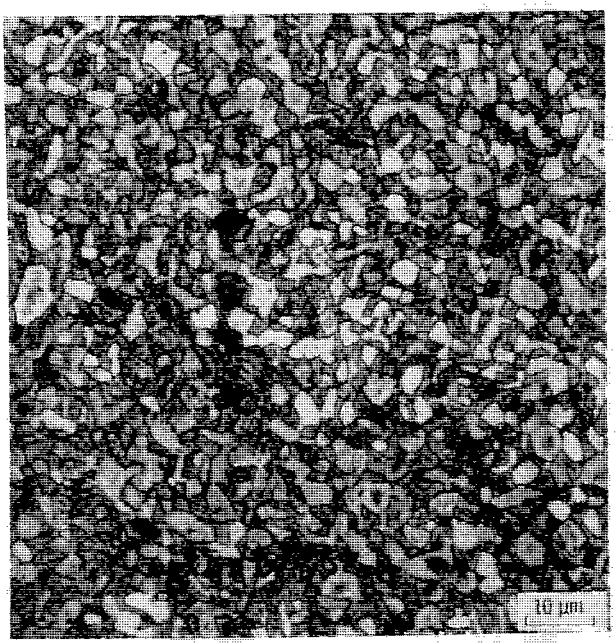

Longitudinal

(f) 64 Duplex.

Figure 8. - Continued.

Transverse

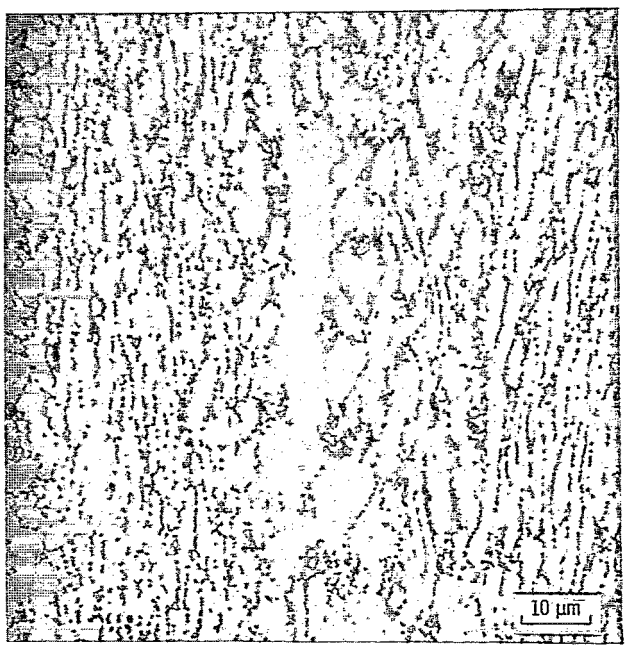

Longitudinal

(g) 6242 Mill anneal.

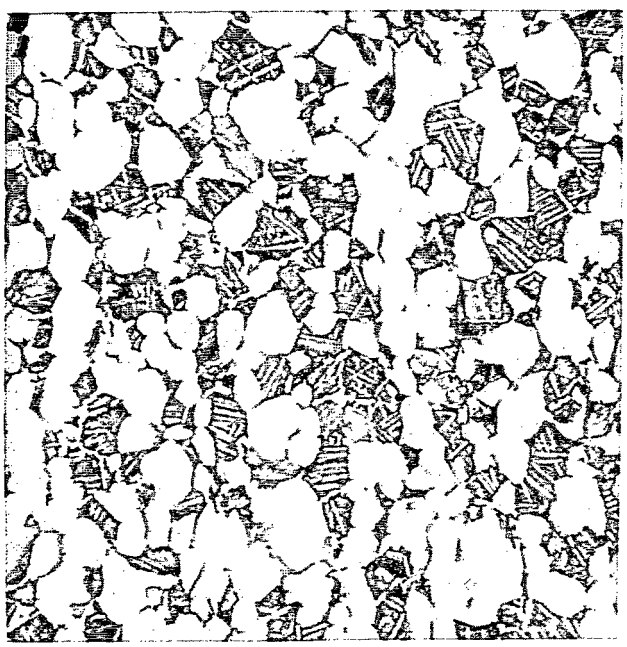

Transverse

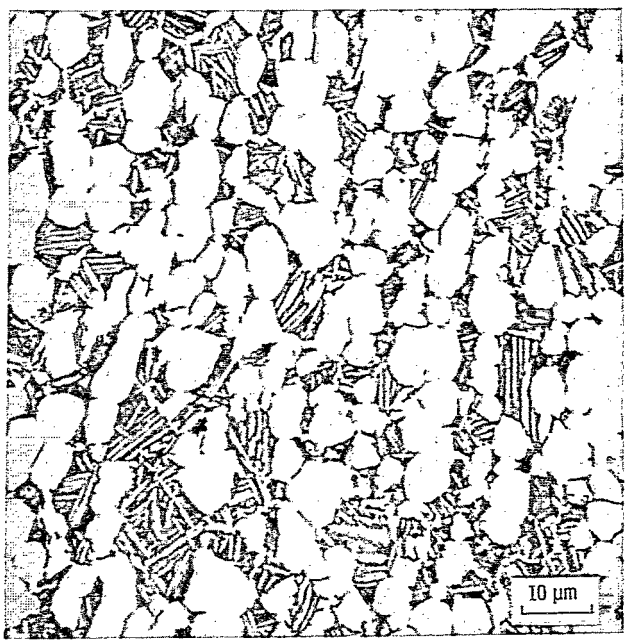

Longitudinal

(h) 6242 Duplex.

Figure 8. - Continued.

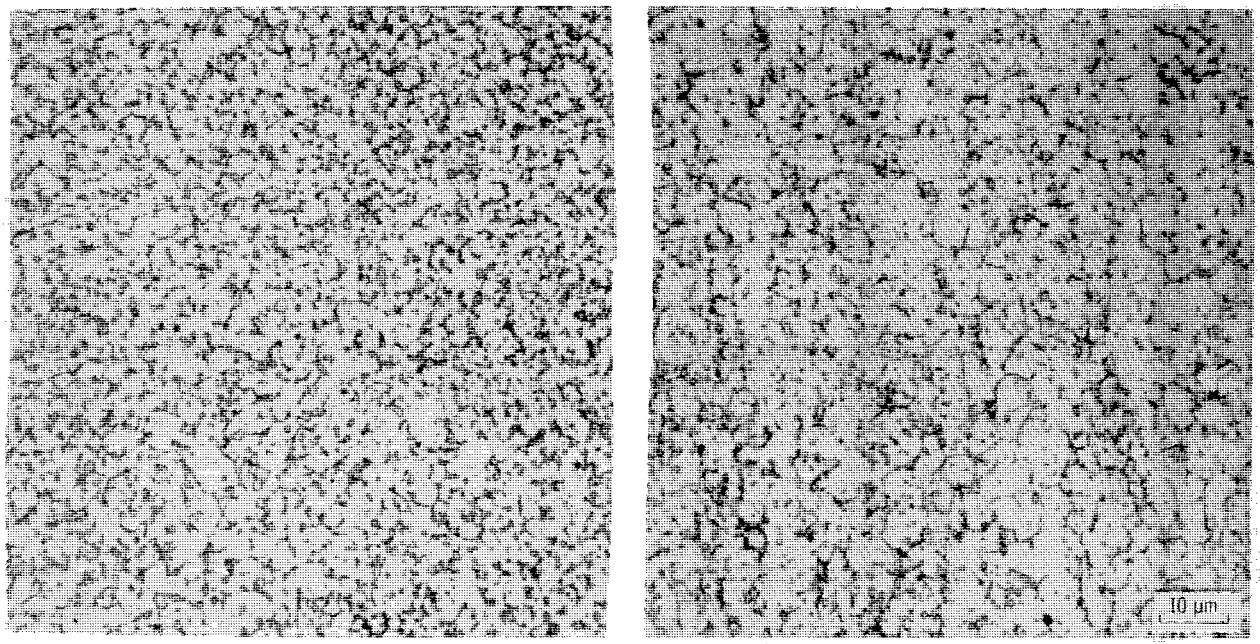

Transverse Longitudinal

(i) 679 Mill anneal.

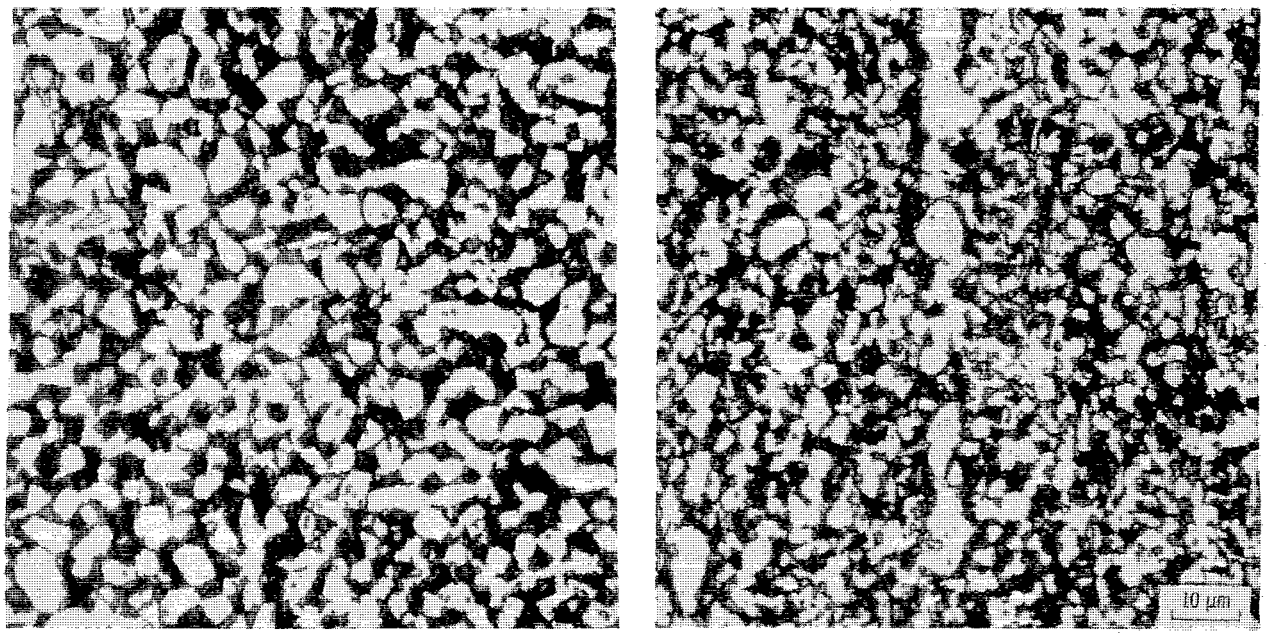

Transverse Longitudinal

(j) 679 Duplex.

Figure 8. - Continued.

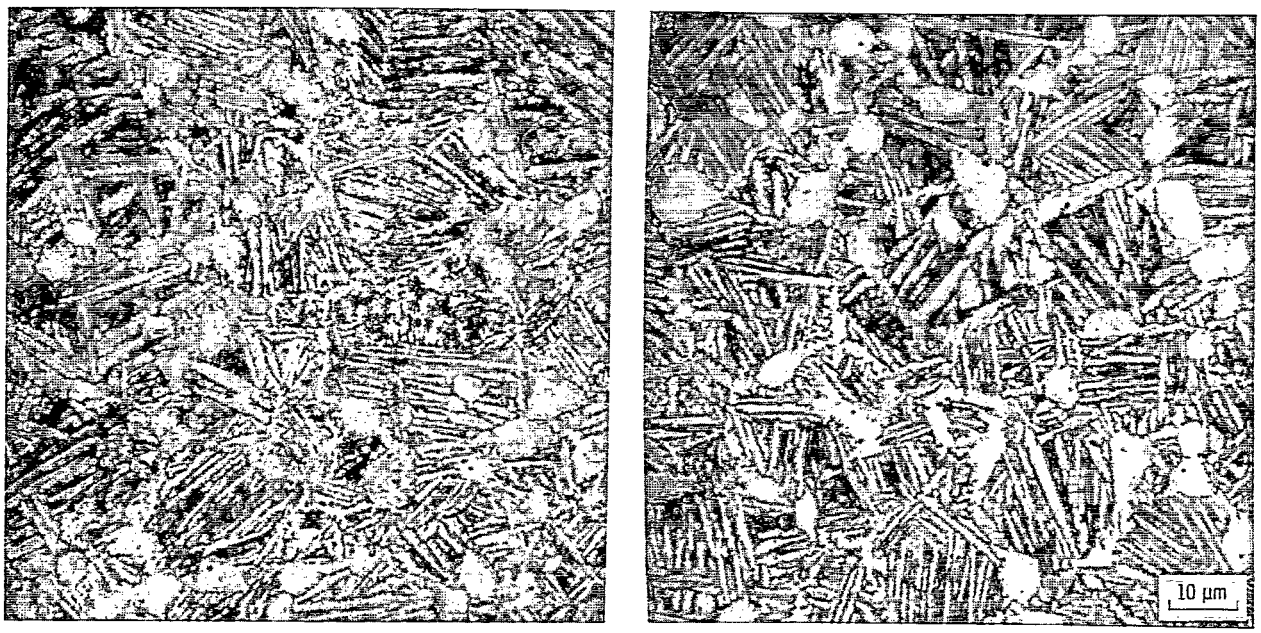

Transverse Longitudinal

(k) 5621S (1).

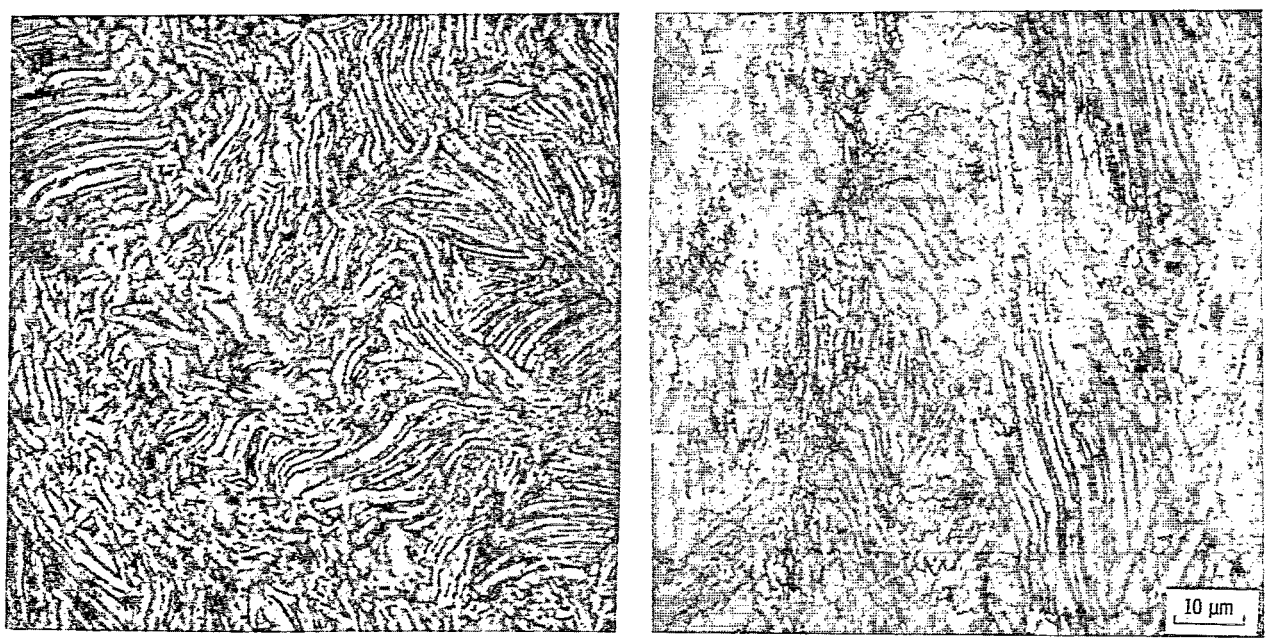

Transverse Longitudinal

(l) 5621S (2A).

Figure 8. - Continued.

Transverse

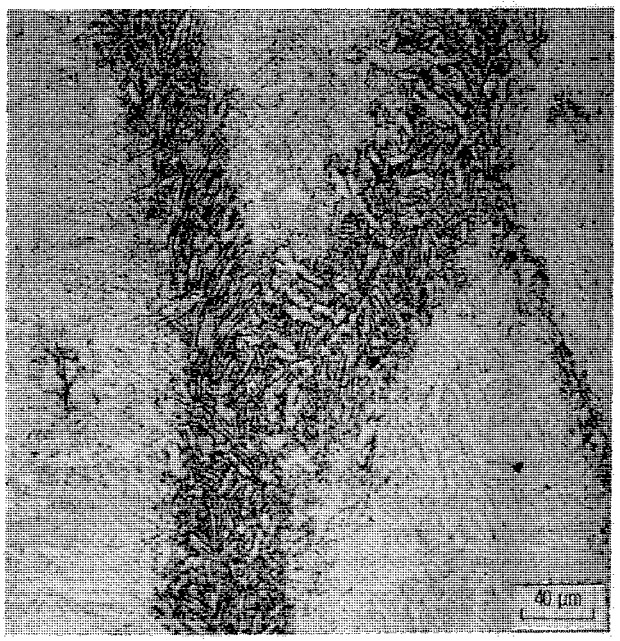

Longitudinal

(m) 5621S (2B).

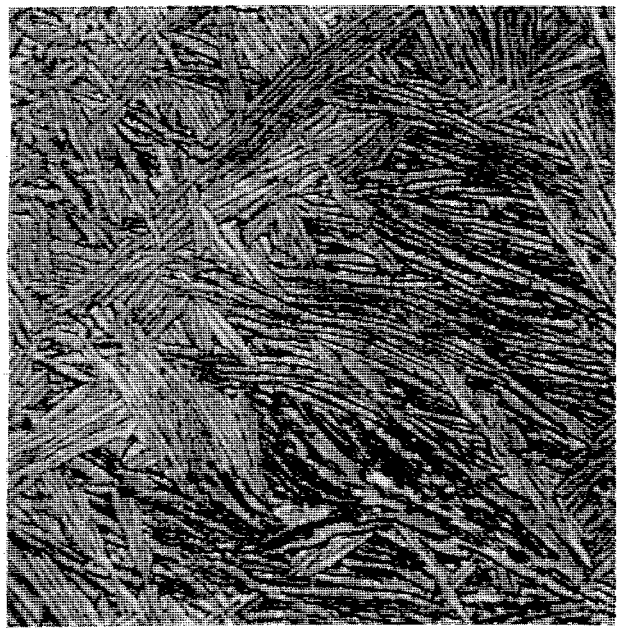

Transverse

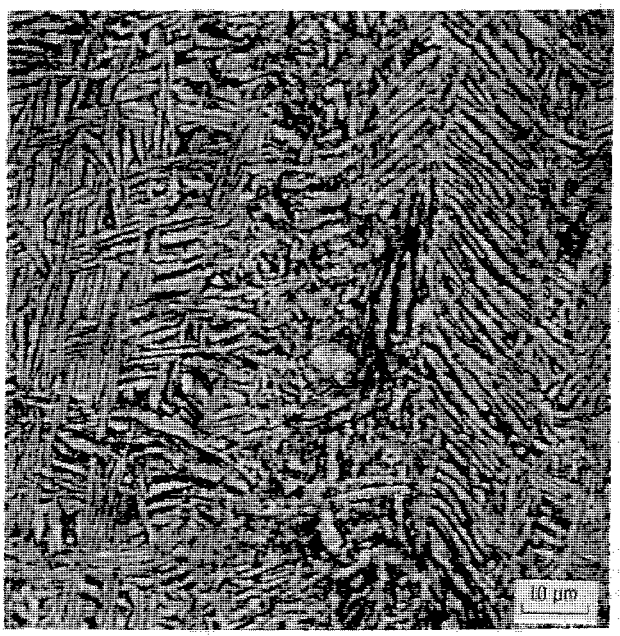

Longitudinal

(n) 5621S (2B).

Figure 8. - Continued.

Longitudinal

(o) 5621S (2C).

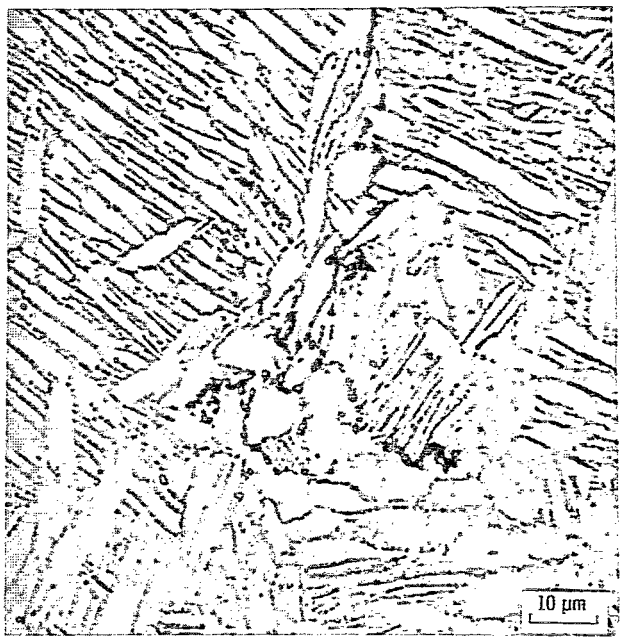

Longitudinal

(p) 5621S (2C).

Transverse

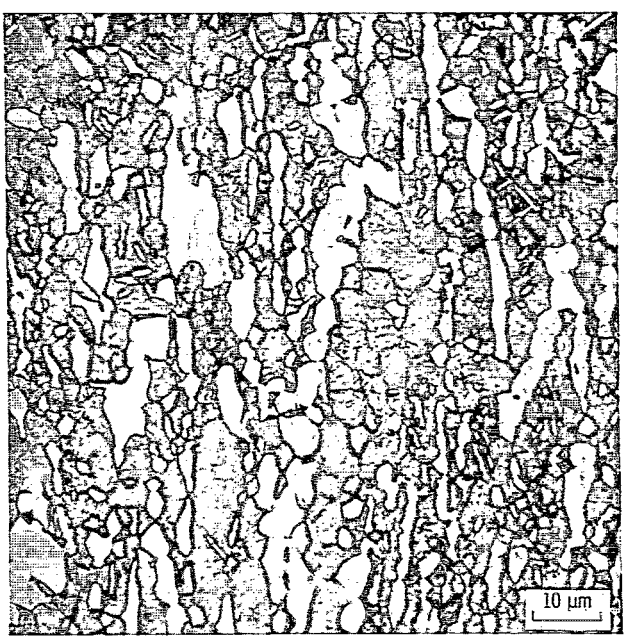

Longitudinal

(q) 643 Duplex.

Figure 8. - Continued.

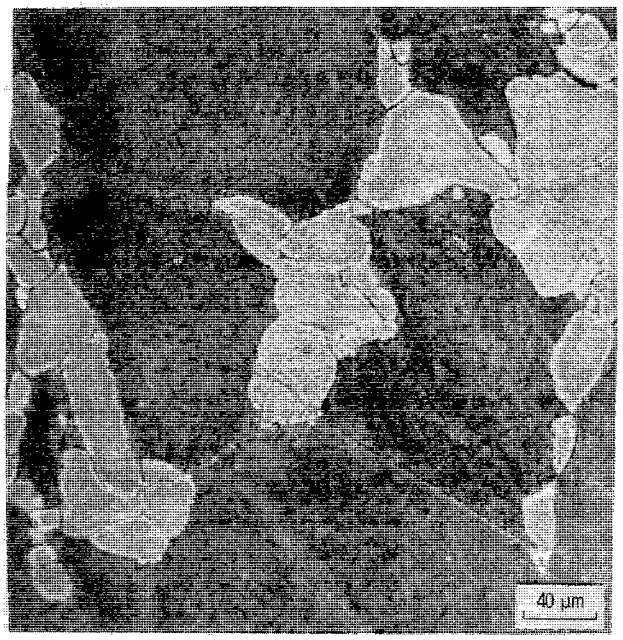

Longitudinal

(r) 13-11-3 Duplex.

Longitudinal

(s) 13-11-3 Duplex.

Figure 8. - Concluded.

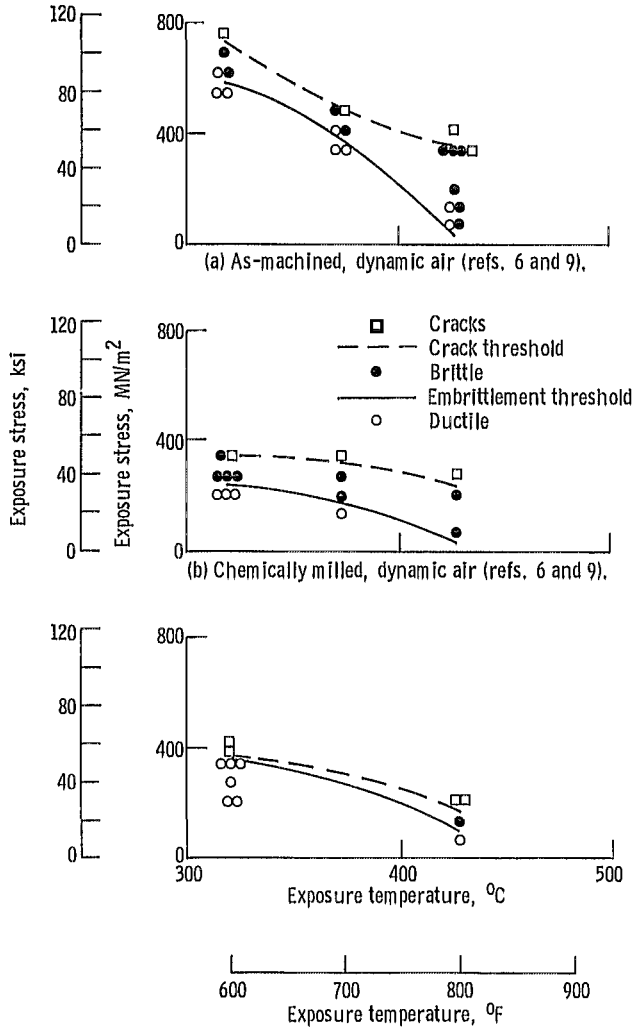

(a) As-machined, dynamic air (refs. 6 and 9).

(b) Chemically milled, dynamic air (refs. 6 and 9).

(c) Chemically milled, static air.

Figure 9. - Threshold curves for 811 mill anneal/air cool (table V).

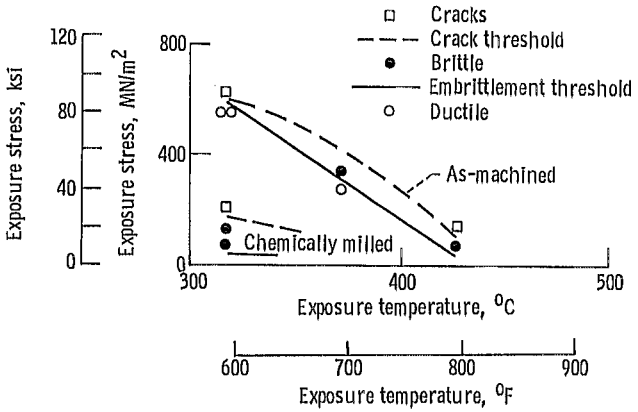

Figure 10. - Threshold curves for 811 mill anneal/furnace cool, dynamic air (table VI).

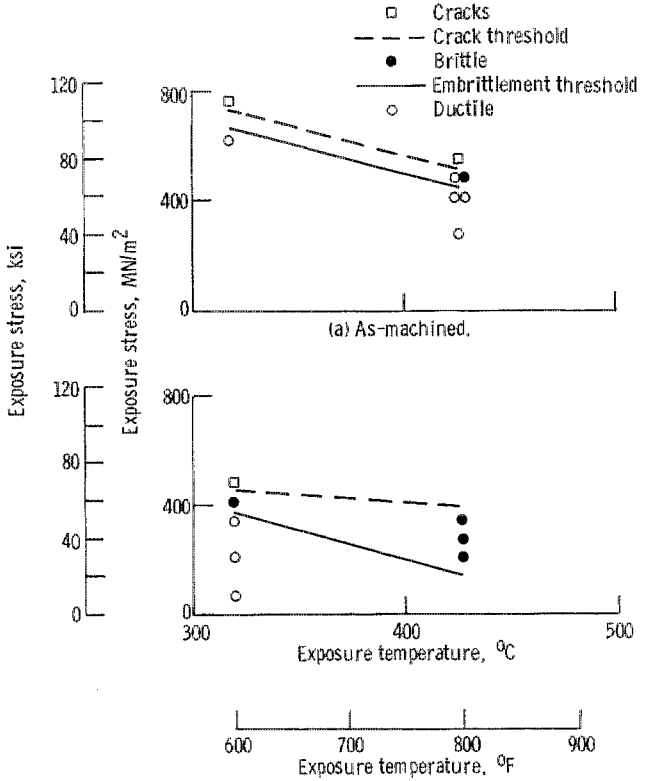

Figure 11. - Threshold curves for 811 duplex, dynamic air (table VII)

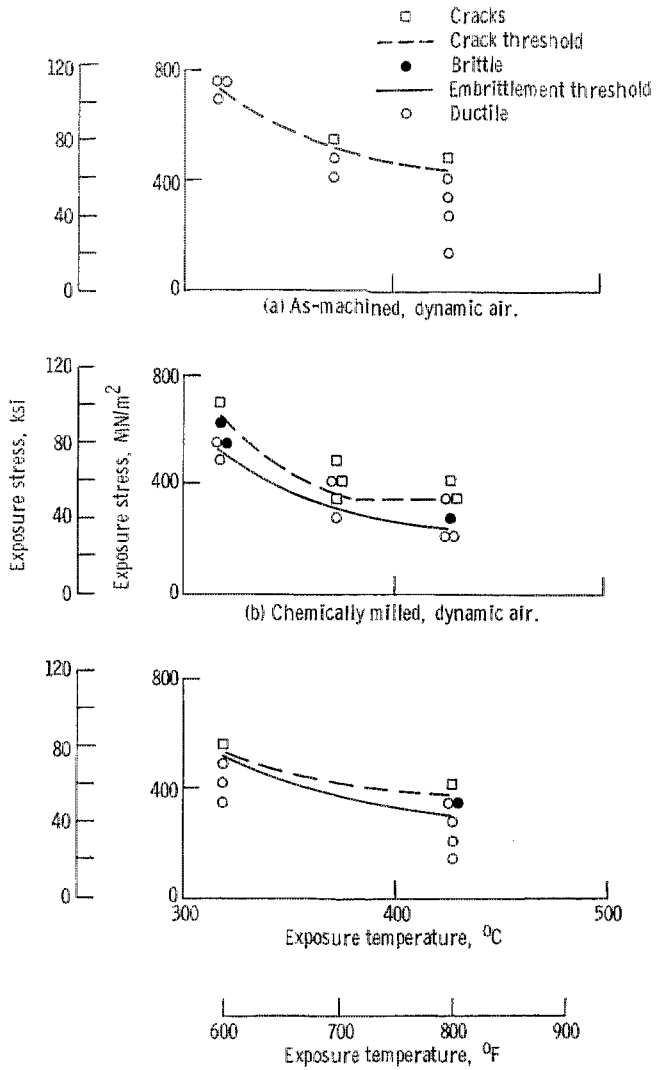

Figure 12. - Threshold curves for 811 triplex (table VIII).

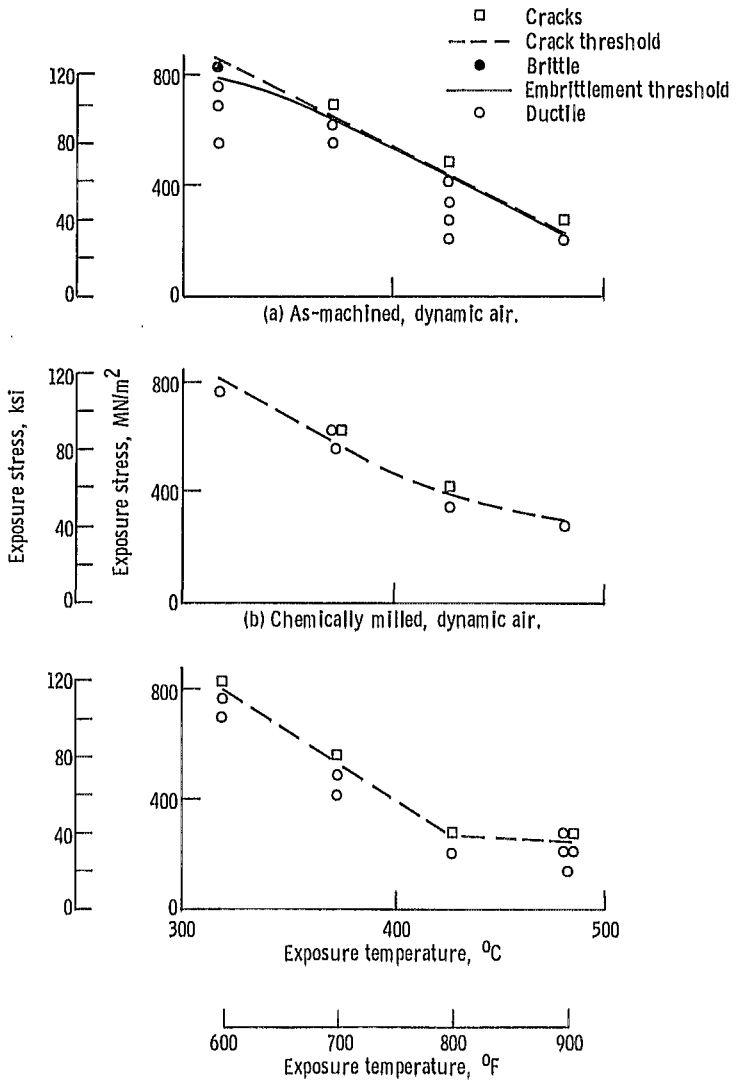

Figure 13. - Threshold curves for 64 mill anneal (table IX).

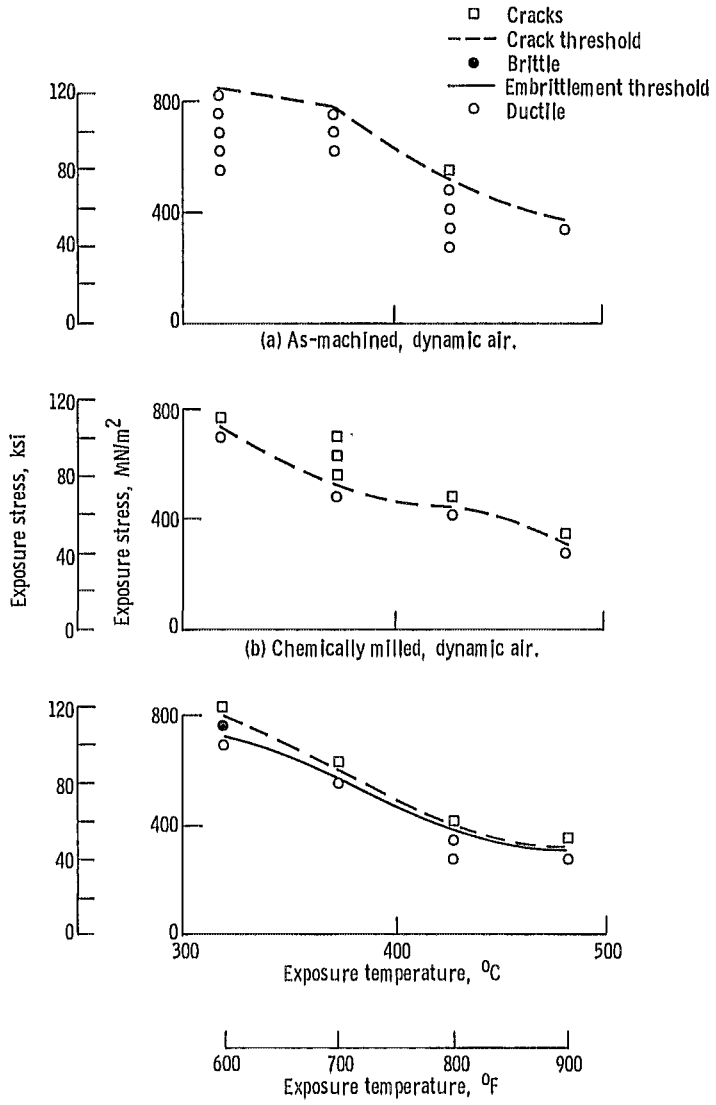

Figure 14. - Threshold curves for 64 duplex (table X).

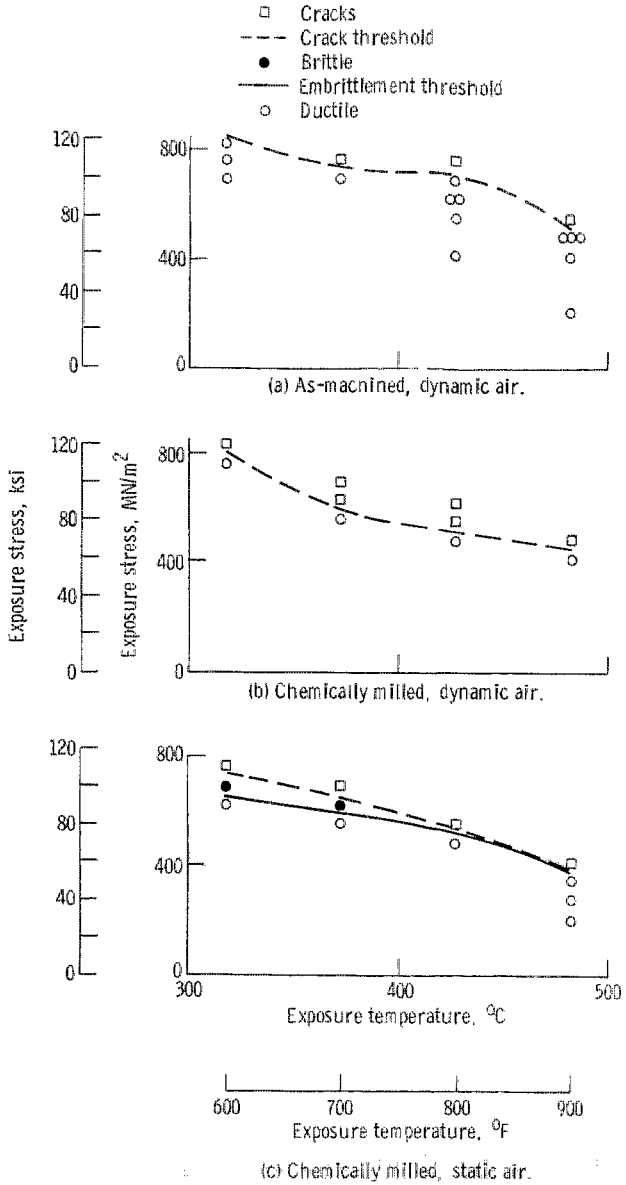

Figure 15. - Threshold curves for 6242 mill anneal (table XI).

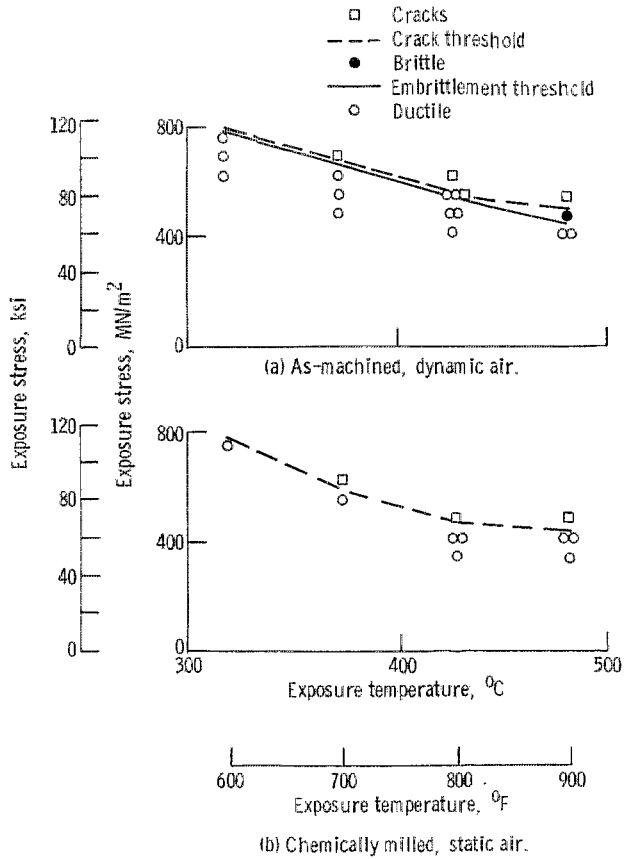

Figure 16. - Threshold curves for 6242 duplex (table XII).

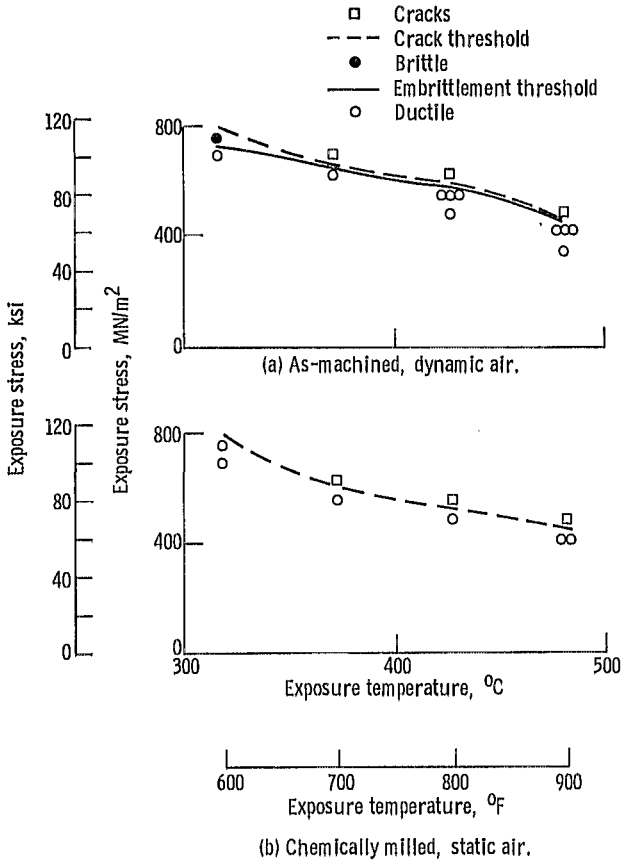

Figure 17. - Threshold curves for 679 mill anneal (table XIII).

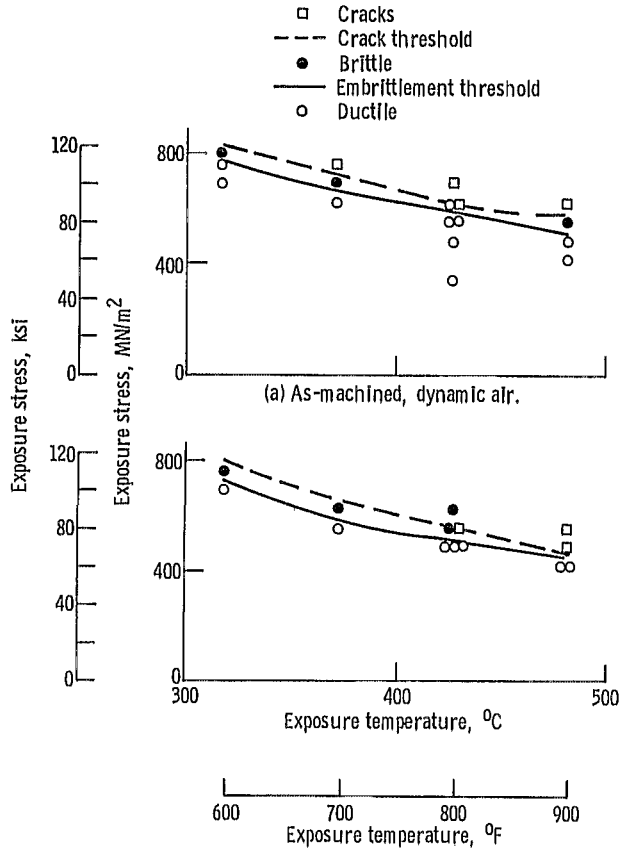

Figure 18. - Threshold curves for 679 duplex (table XIV).

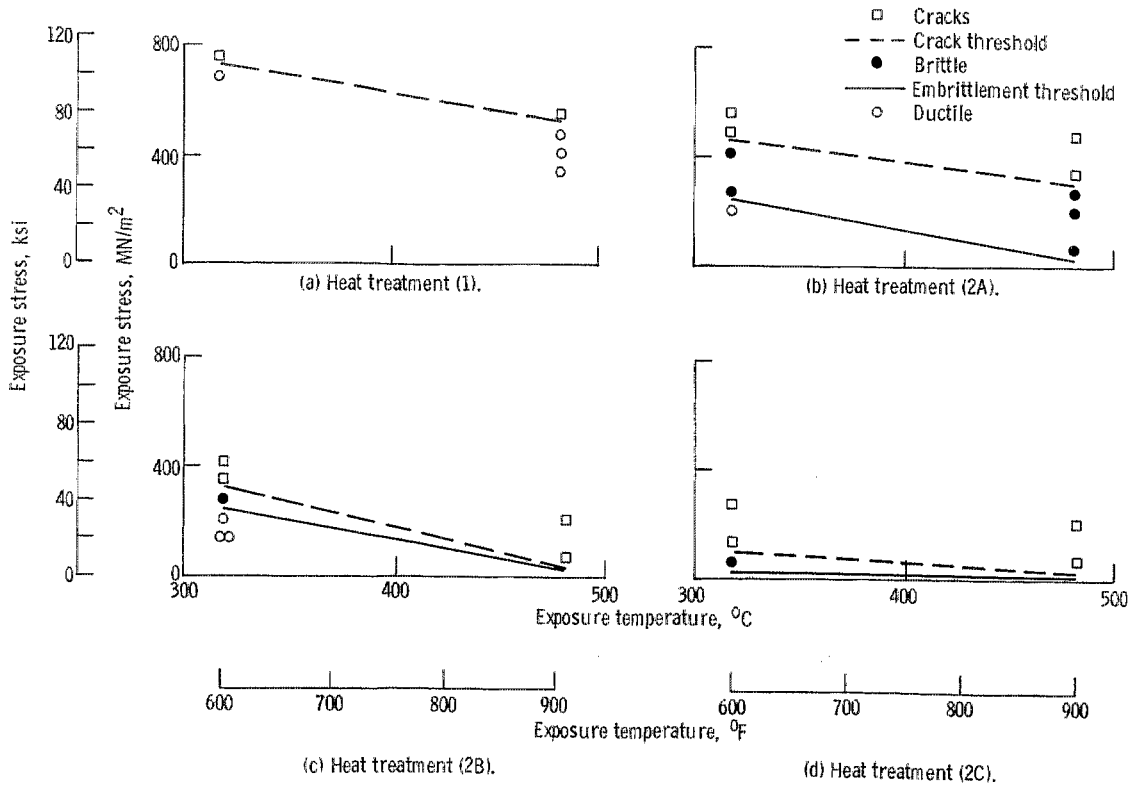

Figure 19. - Threshold curves for 5621S, chemically milled, dynamic air (table XV).

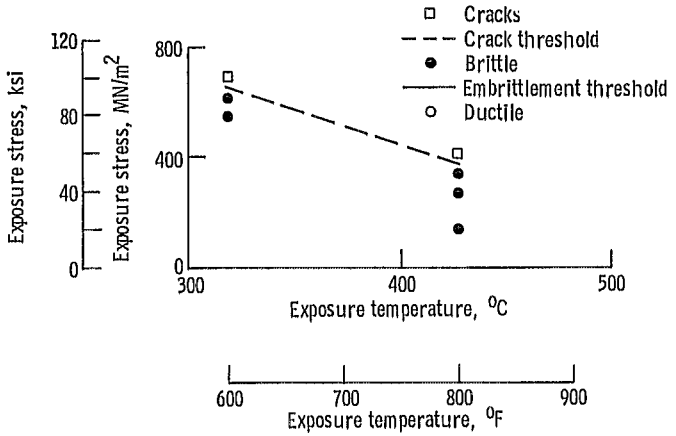

Figure 20. - Threshold curves for 643 duplex, chemically milled, dynamic air (table XVI).

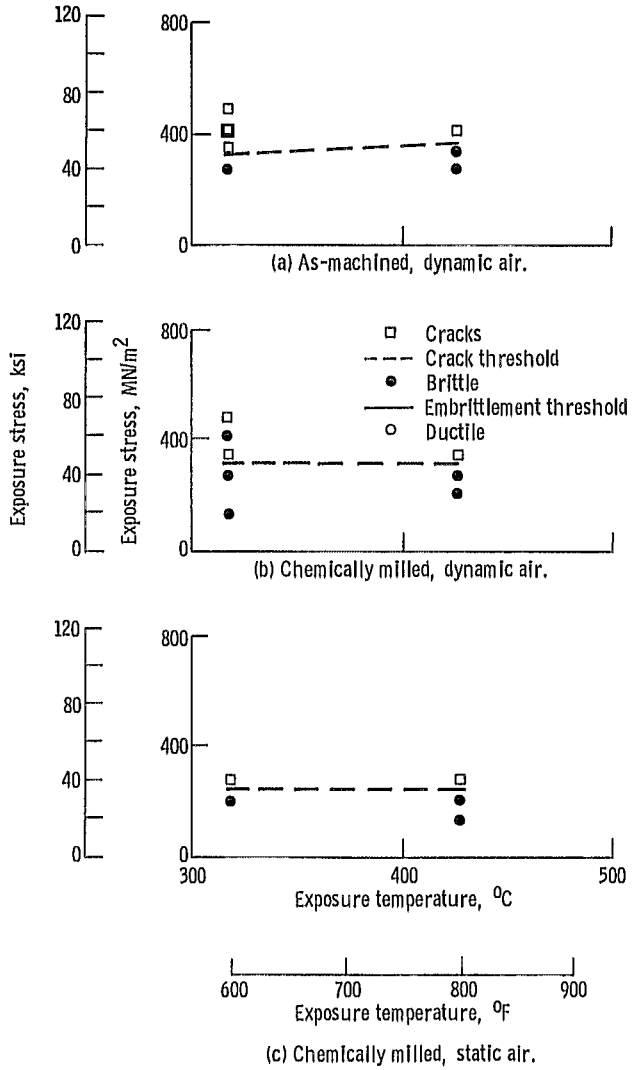

Figure 21. - Threshold curves for 13-11-3 duplex (table XVII).

"The aeronautical and space activities of the United States shall be conducted so as to contribute . . . to the expansion of human knowledge of phenomena in the atmosphere and space. The Administration shall provide for the widest practicable and appropriate dissemination of information concerning its activities and the results thereof."

—NATIONAL AERONAUTICS AND SPACE ACT OF 1958

NASA SCIENTIFIC AND TECHNICAL PUBLICATIONS

TECHNICAL REPORTS: Scientific and technical information considered important, complete, and a lasting contribution to existing knowledge.

TECHNICAL NOTES: Information less broad in scope but nevertheless of importance as a contribution to existing knowledge.

TECHNICAL MEMORANDUMS: Information receiving limited distribution because of preliminary data, security classification, or other reasons.

CONTRACTOR REPORTS: Scientific and technical information generated under a NASA contract or grant and considered an important contribution to existing knowledge.

TECHNICAL TRANSLATIONS: Information published in a foreign language considered to merit NASA distribution in English.

SPECIAL PUBLICATIONS: Information derived from or of value to NASA activities. Publications include conference proceedings, monographs, data compilations, handbooks, sourcebooks, and special bibliographies.

TECHNOLOGY UTILIZATION PUBLICATIONS: Information on technology used by NASA that may be of particular interest in commercial and other non-aerospace applications. Publications include Tech Briefs, Technology Utilization Reports and Technology Surveys.

Details on the availability of these publications may be obtained from:

SCIENTIFIC AND TECHNICAL INFORMATION OFFICE

NATIONAL AERONAUTICS AND SPACE ADMINISTRATION

Washington, D.C. 20546